



**UNIVERSIDADE FEDERAL DO CEARÁ**  
**CENTRO DE TECNOLOGIA**  
**DEPARTAMENTO DE ENGENHARIA HIDRÁULICA E AMBIENTAL**  
**PROGRAMA DE PÓS-GRADUAÇÃO EM ENGENHARIA CIVIL**

**VICTOR COSTA PORTO**

**ADVANCEMENTS IN STREAMFLOW MODELING AND FORECASTING IN  
BRAZIL**

**FORTALEZA**

**2023**

VICTOR COSTA PORTO

ADVANCEMENTS IN STREAMFLOW MODELING AND FORECASTING IN BRAZIL

Tese apresentada ao Programa de Pós-Graduação em Engenharia Civil da Universidade Federal do Ceará, como requisito parcial à obtenção do título de Doutor em Engenharia Civil. Área de concentração: Recursos Hídricos.

Orientador: Prof. Dr. Francisco de Assis de Souza Filho.

Fortaleza

2023

Dados Internacionais de Catalogação na Publicação  
Universidade Federal do Ceará  
Sistema de Bibliotecas

Gerada automaticamente pelo módulo Catalog, mediante os dados fornecidos pelo(a) autor(a)

---

P883a Porto, Victor Costa.  
ADVANCEMENTS IN STREAMFLOW MODELING AND FORECASTING IN BRAZIL / Victor  
Costa Porto. – 2023.  
94 f. : il. color.

Tese (doutorado) – Universidade Federal do Ceará, Centro de Tecnologia, Programa de Pós-Graduação  
em Engenharia Civil: Recursos Hídricos, Fortaleza, 2023.  
Orientação: Prof. Dr. Francisco de Assis de Souza Filho .

1. Previsão Sazonal. 2. Simulação Hidrológica. I. Título.

CDD 627

---

VICTOR COSTA PORTO

ADVANCEMENTS IN STREAMFLOW MODELING AND FORECASTING IN BRAZIL

Tese apresentada ao Programa de Pós-Graduação em Engenharia Civil da Universidade Federal do Ceará, como requisito parcial à obtenção do título de Doutor em Engenharia Civil. Área de concentração: Recursos Hídricos.

Aprovada em: 23/10/2023

BANCA EXAMINADORA

---

Prof. Dr. Francisco de Assis de Souza Filho (Orientador)  
Universidade Federal do Ceará (UFC)

---

Prof. Dra. Ticiania Marinho de Carvalho Studart  
Universidade Federal do Ceará (UFC)

---

Prof. Dr. Eduardo Sávio Passos Rodrigues Martins  
Universidade Federal do Ceará (UFC)

---

Prof. Dr. Luiz Martins de Araújo Junior  
Universidade da Integração Internacional da Lusofonia Afro-Brasileira (UNILAB)

---

Dr. Domingo Cassain Sales  
Fundação Cearense de Meteorologia e Recursos Hídricos (FUNCEME)



Aos meus pais, Adonai e Naila.

## **AGRADECIMENTOS**

Primeiro, preciso agradecer ao meu orientador, o Professor Dr. Francisco de Assis de Souza Filho, não só por sua orientação impecável para a construção desta tese mesmo em tempos sombrios, nem somente pela grande inspiração e exemplo de profissional, mas por todos os conselhos, carões e reflexões e por tudo que consegui aprender durante esses 10 anos de intensa convivência. O jovem de 19 anos que iniciou uma iniciação científica em 2013, sem saber o que gostava ou queria, termina em 2023 aos 29 anos a sua última etapa de formação com satisfação e sabendo o que quer e o seu papel no mundo. Boa parte dessa maturidade, do cientista, do profissional e do ser humano que me tornei se devem à sua convivência, ao seu exemplo e ao ambiente divertido de trabalho que o senhor construiu no GRC. Tenho certeza de que o fim desta tese é o começo de mais uma etapa da nossa convivência, que ainda tenho muito o que aprender e teimar com o senhor e que ainda vamos realizar muitas ideias juntos.

Agradeço à minha família, em especial aos meus pais Adonai e Naila e ao meu irmão Bruno. Jamais teria conseguido sem o incentivo, a motivação e o amor que me propiciam e o conforto que é a nossa família. Muito obrigado por sempre me incentivarem a ser o melhor que posso.

Agradeço a todos os amigos que fiz no GRC e que tornaram essa caminhada mais leve e tranquila, especialmente ao Renan pela grande e sólida amizade que construímos; à Gabi pela amizade e pelo amadurecimento que nossa convivência proporcionou; ao João Dehon pela amizade e pelos bons conselhos sempre que preciso; à Thaís pela amizade e parceria que foram muito importantes nessa reta final, que os bons ventos continuem conduzindo os nossos projetos e planos, vontade e energia sei que não faltarão; e ao Alyson pela amizade, convivência e aprendizado mútuo que conseguimos proporcionar.

Por fim, agradeço também aos amigos da Funceme que me receberam com muito carinho durante o momento mais sensível dessa jornada. Agradeço também pelos bons momentos que me proporcionaram. Apesar do breve período de convivência, foi extremamente significativo, e espero manter esse laço de amizades com todos vocês.

“O Tejo é mais belo que o rio que corre pela  
minha aldeia,

Mas o Tejo não é mais belo que o rio que corre  
pela minha aldeia

Porque o Tejo não é o rio que corre pela minha  
aldeia.” (Fernando Pessoa)

## RESUMO

Esta tese de doutorado apresenta dois avanços significativos na modelagem e previsão de vazão no Brasil. A primeira contribuição está no domínio metodológico, onde é proposta uma nova técnica estatística para a modelagem de vazão em múltiplos locais, chamada GLM-Copula, que combina Modelos Lineares Generalizados (GLM) para representar as dependências temporais e a Copula para representar as dependências espaciais. Essa técnica permite modelar estruturas de dependência usando várias funções de probabilidade, eliminando assim a necessidade de normalização. Os resultados mostraram que a abordagem GLM-Copula possui habilidade semelhante aos modelos multivariados ARMA clássicos e aos modelos COPAR de última geração em preservar as estatísticas resumidas dos dados históricos. O modelo proposto permite a modelagem de dependências espaciais e temporais sem normalização, é computacionalmente eficiente e pode ser usado como uma redução dimensional, o que justifica sua adição à caixa de ferramentas de geração de séries temporais. A segunda contribuição desta tese está no domínio da literatura de previsão dinâmica sazonal de vazões, onde é aplicada uma abordagem probabilística multimodelo para a previsão sazonal das vazões em todos os 87 reservatórios hidrelétricos brasileiros monitorados pelo ONS. Essa contribuição busca preencher a lacuna na literatura científica de previsão sazonal dinâmica de vazão no Brasil, propondo uma abordagem de conjunto de modelos múltiplos para gerar previsões probabilísticas mensais de vazão a partir de um modelo hidrológico forçado por previsões tanto do NMME quanto do SUBX. Os resultados deste estudo demonstram que a combinação de vários modelos de previsão em uma abordagem de previsão de probabilidade multimodelo apresenta um desempenho melhor e maior robustez em comparação com modelos individuais, incluindo o melhor modelo individual para cada reservatório. Esses resultados foram válidos para a previsão de vazão em todas as regiões do Brasil.

**Palavras-chave:** Previsão sazonal; Simulação Hidrológica; Vazão; Multimodelo; Previsão de conjunto.

## ABSTRACT

This doctoral thesis introduces two significant advancements in streamflow modeling and forecasting in Brazil. The first contribution lies in the methodological domain, wherein a novel statistical technique for multisite streamflow simulation is proposed, the GLM-Copula which couples Generalized Linear Models (GLM) to represent the temporal dependencies and the Copula to represent the spatial dependencies. This technique enables the modeling of dependence structures using various probability functions, thus eliminating the need for normalization. The results showed that the GLM-Copula approach ability to preserve summary statistics from the historical data was similar to the classical multivariate ARMA and the state-of-art COPAR models. For the dependency structures, the GLM-Copula reproduced what was narrowly the best in reproducing the short-term temporal dependence (lag-1 autocorrelation), narrowly the worst in reproducing the spatial dependence (lag-0 cross-correlation) and reasonable the best in reproducing the total association (copula entropy). The proposed model allows the modelling of both spatial and temporal dependencies without normalization, is computationally efficient and can be used as a dimensional reduction, which we suggest justifies its addition to the time series generation toolbox. The second contribution of this thesis lies in the dynamic streamflow forecasting literature domain, where a multimodel probabilistic approach for seasonal streamflow forecasting is applied for all Brazilian hydropower catchments. This contribution seeks to fill the scientific literature gap in dynamic seasonal streamflow forecasting in Brazil by proposing a mutilmodel ensemble approach to generate monthly probabilistic streamflow forecasts from a hydrological model forced by both NMME and SUBX predictions for all the 87 hydropower catchments that are monitored by the electrical system's operator in Brazil. The findings of this study demonstrate that the combination of multiple forecast models into a Multimodel probability forecasting approach yields improved performance and greater robustness compared to individual models, including the best individual model for each catchment. These results hold true for streamflow forecasting across all Brazilian regions.

**Keywords:** Seasonal Forecas; Hidrological Simulation; Streamflow; Multimodel; Ensemble Prediction.



## SUMÁRIO

<b>1</b>	<b>INTRODUÇÃO .....</b>	<b>1</b>
<b>2</b>	<b>A GLM COPULA APPROACH FOR MULTISITE ANNUAL STREAMFLOW GENERATION .....</b>	<b>5</b>
<b>3</b>	<b>DYNAMIC MONTHLY STREAMFLOW FORECASTING. THE BRAZILIAN HIDROELETRIC SECTOR CASE STUDY .....</b>	<b>37</b>
<b>4</b>	<b>CONCLUSION .....</b>	<b>72</b>
<b>5</b>	<b>REFERENCES .....</b>	<b>74</b>





## 1 INTRODUCTION

In Brazil, a country heavily reliant on hydropower, the availability of accurate information regarding future streamflow events is important for effective water and energy management, as well as the optimization of operational costs. The ability to enhance the reliability of streamflow forecasts through advancements in modeling techniques can bring socioeconomical benefits (Boucher et al., 2012; Matte et al., 2017; Cassagnole et al., 2021).

This doctoral thesis endeavors to introduce substantial advancements in the realm of streamflow modeling and forecasting within the context of Brazil. Through the pioneering strides detailed in this research, several imperative aspects of streamflow prediction are poised for enhancement.

The significance of refining streamflow forecasts cannot be overstated. These forecasts hold a pivotal role in water resource management, flood mitigation, agricultural planning, hydropower generation, drought adaptation and mitigation. Accurate streamflow predictions empower decision-makers, policy planners, and stakeholders to make informed choices that directly impact socio-economic stability, environmental sustainability, and public safety.

By refining streamflow modeling and forecasting practices in Brazil, this doctoral thesis takes strides toward addressing gaps in existing knowledge, optimizing predictive accuracy, and fostering a more comprehensive understanding of the intricate relationships between climatic drivers, hydrological systems, and resultant streamflow dynamics.

The first scientific contribution of this thesis lies in the methodological domain, wherein a novel statistical technique for multisite streamflow simulation is proposed. This technique enables the modeling of dependence structures using various probability functions, thus eliminating the need for normalization.

The first contribution is presented in the form of an article named “A GLM COPULA APPROACH FOR MULTISITE ANNUAL STREAMFLOW GENERATION” (Porto et al., 2021). The methodological contribution is a new method for simulating multisite annual

streamflow that couples Generalized Linear Models (GLM) and Copulas distributions, the first to represent the temporal structure and the second, to model the spatial dependence (i.e. the joint distributions). The proposed model exploits both methods' flexibility and synergy: the copula provides a flexible way for estimating the joint distribution that GLM needs for multisite generation; while the GLM lowers the problem's dimension and allows copula models to be applied without the need for normalized data.

The methodology was presented for the Jaguaribe-Metropolitano basin in Ceará, Brazil. Instead of dealing with a hydropower catchment, this article proposed a statistical method for streamflow simulation that could work even in a challenging region - the Ceará State catchments where due to shallow soils, the streamflow series present low short-term time dependency. Although the method was developed for annual streamflow and for streamflow simulation, it can be easily extended for forecasting monthly streamflow.

The second contribution is presented in the form of the article named "DYNAMIC SEASONAL STREAMFLOW FORECASTING. THE BRAZILIAN HIDROELETRIC SECTOR CASE STUDY". Where a multimodel dynamic seasonal streamflow forecast method is presented for forecasting streamflow in the Brazilian electric sector basins. An analysis of the scientific literature pertaining to streamflow forecasting in Brazil during the period from 2014 to 2023 revealed a notable gap in research. Specifically, no dynamic streamflow forecasting articles were found that specifically applied their methodologies at a national level for Brazil. This dearth of national-level dynamic streamflow forecasting studies indicates a significant area where further research is warranted to advance the understanding and practice of streamflow prediction in the Brazilian context.

Moreover, an exploration of the literature within the same timeframe has brought to light a mere five articles focused on dynamic streamflow forecasting (Fan et al., 2015; Fan et al., 2016; Quedi and Fan, 2020; Ávila et al., 2023; Greuell and Hutjes, 2023). Despite their scarcity,

these articles collectively delve into the applicability, robustness, and overall performance of dynamic streamflow forecasts within specific Brazilian catchments. These studies illuminate the value of dynamic forecasting as a pivotal tool for accurate streamflow predictions. Nonetheless, it's important to note that these investigations are confined to regional contexts and single-climate models, rather than encompassing a comprehensive multimodel ensemble approach on a national scale.

While the focus of the second article is to fill the existing literature gap in dynamical monthly streamflow modeling, it also tried to bring some advances that haven't been tried for forecasting streamflow in Brazil like a strategy to optimize weights of models to compose a multimodel probability forecast and the evaluation of subseasonal rainfall models at monthly and national scale. The emphasis on the monthly scale aligns with its significance in forecasting for the management of the electric sector in Brazil.

## **1.1 Objective**

The main objective of this thesis is to advance the understanding of modeling and forecasting streamflow in Brazil by providing a new statistical framework and the evaluation of dynamic seasonal streamflow forecasting in Brazil with state of art techniques.

## **1.2 Specific Objectives**

Specifically, it aims to:

- Develop a flexible multisite annual streamflow generation model that couples GLM and copula.
- Propose a mutimodel ensemble approach to generate monthly probabilistic streamflow forecasts from a hydrological model forced by both NMME and SUBX predictions for all the 87 hydropower catchments that are monitored by the electrical system's operator in Brazil.



## 2 A GLM COPULA APPROACH FOR MULTISITE ANNUAL STREAMFLOW GENERATION<sup>1</sup>

### 1. INTRODUCTION

Synthetic streamflow time series generation has an important role in water resources planning and management. It is applied to the design of reservoir systems and to the definition of their optimal operation rules, to drought evaluation and to several other studies with a stochastic nature (McMahon et al., 2006; Rajagopalan et al., 2010; Salas and Lee, 2010). For a correct application, the generated synthetic series must preserve key historical data characteristics, such as statistical moments and dependence structure (e.g. auto and cross-correlation) (Zachariah and Reddy, 2013).

The classical methods for streamflow simulation, such as the ARMA models (Box and Jenkins, 1976), are based on rigid assumptions about the variables' dependence and require them to follow a Gaussian distribution (Sharma and O'Neill, 2002; Prairie et al., 2006). However, some hydrological variables are significantly skewed which requires their normalization, i.e. their transformation into alternatives variables that satisfy those models' assumptions (Salas et al., 1980; Salas, 1993). Most of those models' drawbacks arise from their rigid assumptions (e.g. the Gaussian) and from the limitations of the data transformation techniques resulting in a lack of flexibility that may influence the preservation of the historical characteristics (Sharma et al., 1997; Prairie et al., 2006; Rajagopalan et al., 2010; Hao and Singh, 2011; Lee and Salas, 2011; Pereira et al., 2017).

The stochastic streamflow simulation literature presents several non-Gaussian modeling alternatives. The most famous are the Lag-1 Gamma Autoregressive model (GAR-1)

---

<sup>1</sup> Article published as: Porto, V. C., de Souza Filho, F. D. A., Carvalho, T. M. N., de Carvalho Studart, T. M., & Portela, M. M. (2021). A GLM copula approach for multisite annual streamflow generation. *Journal of Hydrology*, 598, 126226.

(Fernandez and Salas, 1990) and the nonparametric approaches such as the K-Nearest Neighbor method (KNN) (Lall and Sharma, 1996), and the Kernel Density Estimators (KDE) (Sharma et al., 1997; Sharma and O'Neill, 2002). However, these alternative models have their own limitations. The GAR-1 also lacks flexibility and cannot model long term persistency. Furthermore, resampling methods, like the KNN, reproduce only the observed values and the KDE may not be applied to higher dimensions (Rajagopalan et.al., 2010; Lee and Salas, 2011).

Recently, copula based approaches have been applied to hydrologic time series generation (Lee and Salas, 2011; Zachariah and Reddy, 2013; Chen et al., 2015; Pereira et al., 2017). The copula methods are parametric approaches that model the dependence structure apart from the marginal distributions, which provides high flexibility by allowing the use of any marginal distributions. Lee and Salas (2011) compared the performance of a copula and an ARMA model applied to single site annual streamflow generation and showed the former had some benefits, if small.

Generalized Linear Models (GLMs), introduced by Nelder and Wedderburn (1972) as an extension of the classical linear regression model, are parsimonious parametric methods that allow the modelling of non-Gaussian variables (McCullagh and Nelder, 1989). As stated by Rajagopalan et al. (2010), GLM approaches may be reasonable alternatives to the traditional parametric methods due to their flexibility and capability to preserve different features of the historical series.

The use of GLMs is recognized in hydrology for stochastic generation of daily weather variables, like precipitation, temperature, and potential evapotranspiration (Chandler and Wheeler, 2002; Chandler, 2005; Yang et al., 2005; Wheeler et al., 2005; Furrer and Katz, 2007; Kleiber et al., 2012; Verdin et al., 2015). However, to the knowledge of the authors, GLMs have not yet been applied for streamflow stochastic generation.

Thus, the first part of this research addresses the applicability of GLM to generate single site annual streamflow and compares its ability to model temporal dependence and preserve historical statistics against a traditional univariate autoregressive (AR) method.

For multisite time series generation, GLM approaches require the specification of the joint probability distributions of the time series which is obtained from a spatial dependence modelling that respects the marginal distributions (Yang et al., 2005). However, modelling the spatial structure is a complex process that is often done in the GLM-based weather generators by multivariate Gaussian assumptions that may need data normalization, reducing the approach's flexibility (Yang et al., 2005; Kleiber et al., 2012; Verdin et al., 2015).

Meanwhile, high dimensional copulas ( $d \geq 3$ ) lose their flexibility to represent the dependence structures as there is a limited set of higher dimensional copula families (Kao and Govindaraju, 2008; Aas et al., 2009; Hao and Singh, 2013). To overcome this limitation, recent copula times series models are mostly built from two approaches: i) vine copulas that decomposes the multidimensional problem into a sequence of bidimensional copulas (Brechmann and Czado, 2015; Pereira et al., 2017; Wang et al., 2018) or ii) maximum entropy copula that based on the concept of maximum entropy distribution from the information theory can fit a flexible high dimensional copula (Hao and Singh, 2013; Hao and Singh, 2015; Singh and Zhang, 2018;). However, the complexity and the computational burden grows quickly with the dimension for both entropy and vine copula models (Hao and Singh, 2015; Pereira et al., 2017).

The second part of this research presents a multisite annual streamflow generation model that couples GLM and copula, the first to represent the temporal structure and the second, to model the spatial dependence (i.e. the joint distributions). Its performance to reproduce historical statistics and dependence structures is compared with the traditional multivariate ARMA model and the copula autoregressive (COPAR) model (Brechmann and Czado, 2015),

a state-of-art copula time series model that extends the vine copula concept to model both spatial and temporal dependence.

The proposed model exploits both methods' flexibility and synergy: the copula provides a flexible way for estimating the joint distribution that GLM needs for multisite generation; while the GLM lowers the problem's dimension and allows copula models to be applied without the need for normalized data.

Despite the existence of several stochastic multisite streamflow time series generation methods, none is universally accepted (Srinivas and Srinivasan, 2005; Chen et al., 2015; Hao and Singh, 2016). In contrast, the proposed model allows us to model both spatial and temporal dependencies without normalization, is computationally efficient and can be used as a dimensional reduction, for vine and maximum entropy copula practitioners, which we suggest justifies its addition to the time series generation toolbox.

## **2. CASE STUDY, DATA AND PRELIMINARY ANALYSIS**

In this paper, the Jaguaribe-Metropolitano reservoir system in Ceará State (Brazil), represented in Figure 1, was selected as the multi-site synthetic flow series generation case study, since the annual inflows at its seven reservoirs are highly variable and skewed (Souza Filho and Lall, 2003). The annual inflow data to those reservoirs are available for the 1912-2012 period (101 years) from Barros et al. (2013).

The Jaguaribe-Metropolitano is the State's greatest water impounding system and the most important water supply source. It comprises two different basins, the Jaguaribe and the Metropolitano basins, with 72000 and 15200 km<sup>2</sup> respectively, that were artificially connected by channels allowing the latter to receive water from the former. Most of the system is located in a semiarid region with a highly variable annual streamflow, due to the temporal variability of the precipitation and the predominance of shallow soils (Silva et al., 2017).

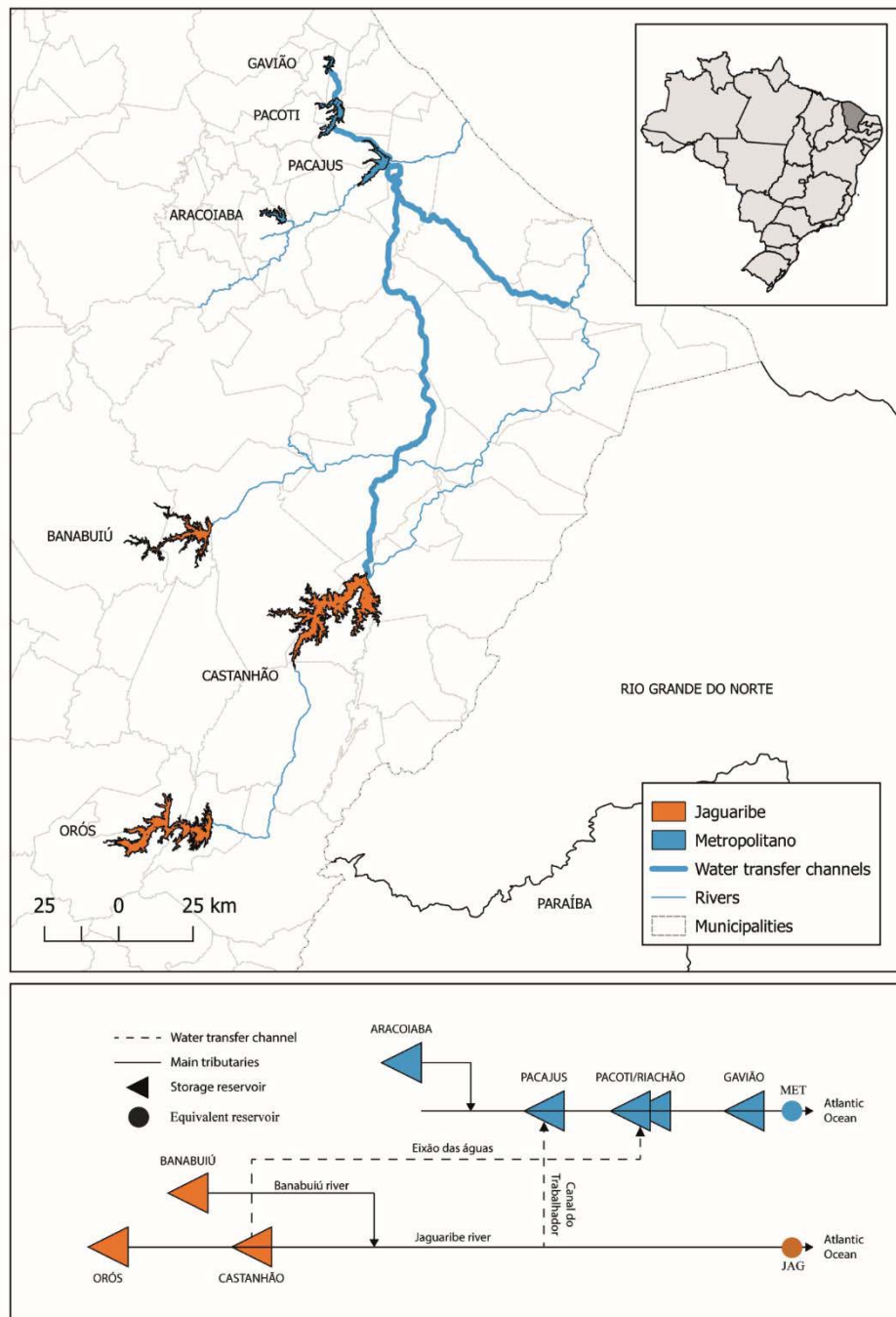
The Jaguaribe basin covers approximately 48% of the State of Ceará and its main water



use is irrigation which accounts for about 90% of the state agricultural production. Although the Metropolitan basin is smaller, comprising approximately 10% of the State area, it has a larger population and supplies water to the capital city (Fortaleza) and to its metropolitan region for domestic supply, industry, and tourism. The water demand in the Metropolitan basin is almost uniform throughout the year while the one in Jaguaribe basin is concentrated in the second semester due to the crop irrigation period (i.e. the dry station) (Souza Filho and Lall, 2003; Silva et al., 2017).

The system is composed of seven major reservoirs (from upstream to downstream): Orós, Castanhão, Banabuiú, Aracoiaba, Pacajus, Pacoti and Gavião. The first three are in the Jaguaribe basin and the last four are in the Metropolitan basin (total storage capacity of 10,240 and 871 hm<sup>3</sup>, respectively) (Figure 1). For water resources planning and management purposes, the Jaguaribe-Metropolitan system can be represented as two equivalent reservoirs, one for each basin, located at the most downstream sections of the main rivers of Jaguaribe and the Metropolitan basins, as illustrated in Figure 1. In this research, the annual inflows to the Jaguaribe (JAG) and Metropolitan (MET) equivalent reservoirs were obtained by summing the annual inflows to each of their major component reservoirs.

Figure 1- The Jaguaribe-Metropolitan reservoir system in Ceará, Brazil.



The temporal correlation and the spatial cross-correlation of the annual inflows series thus obtained for JAG and MET are characterized in Figure 2 for lags 0 until 17.

In spatial terms, there is a high lag-0 correlation ( $>0.8$ ), as shown by the cross-correlation function, because the rainfall regime in both basins mainly relies on the same climatic process: the Intertropical Convergence Zone (ITCZ) displacement (Moura and Shukla,

1981; Andreoli and Kayano, 2004; Wang et al., 2004).

In temporal terms, both series present a short-term persistency pattern with a fast correlogram decay after the first lag. There is also a long-term dependence pattern with significant positive correlation coefficients for lags 10 and 11. The short memory pattern may be a result of low groundwater flow, since both basins are situated in a crystalline Precambrian basement with shallow soils and poor vegetation cover (Frischkorn et al., 2003; Alexandre et al., 2005; Barros et al., 2013). The long-term persistency may be related to a decadal sea surface temperature variability in the Tropical Atlantic that influences the ITCZ location (Andreoli and Kayano, 2004; Andreoli and Kayano, 2006).

The empirical and fitted cumulative distribution functions (CDF) and probability density functions (PDF) of the annual flows at each equivalent reservoir are shown in Figure 3, showing convincing similarity both series are non-Gaussian and right-skewed. The inflows to JAG are close to a lognormal distribution and those to MET, to a gamma distribution. The selection of the best-fit distribution was based in the Anderson-Darling test for the maximum likelihood estimated parameters and the fit of the CDFs is remarkably good throughout the range of data.

Figure 2 - Temporal autocorrelation (top-left and bottom-right) and spatial cross-correlation (top-right and bottom-left) functions of the annual streamflow series of the JAG and MET equivalent reservoirs. The dashed lines represent the 95% confidence intervals.

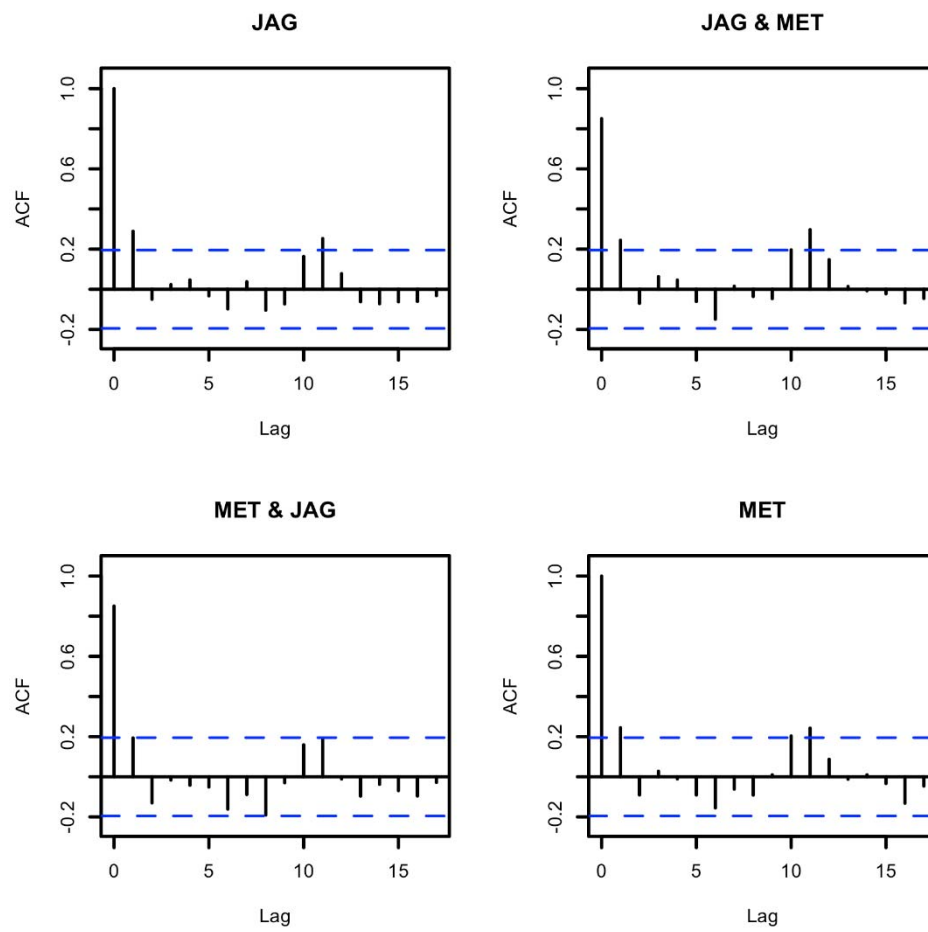
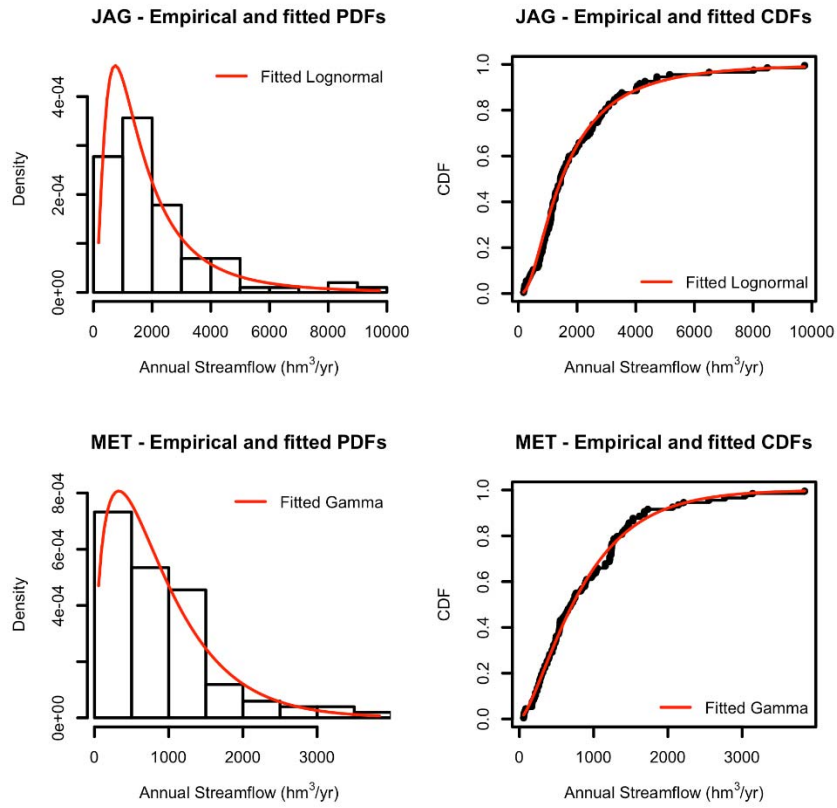


Figure 3 – Empirical and fitted probability density (PDF) and cumulative distribution (CDF) functions of the annual streamflow series at the JAG (top) and MET (bottom) equivalent reservoirs. Note that preferably Lognormal fits JAG and Gamma fits MET.



### 3. BACKGROUND AND METHODOLOGY

#### 3.1. Generalized Linear Models

The classical linear regression model is defined as:

$$y_i = \alpha + \beta x_i + \varepsilon_i \quad \varepsilon_i \sim N(0, \sigma^2) \quad i = 1, \dots, n \quad (1)$$

where,  $y_i$  is each value of the response variable,  $\alpha$  is the intercept,  $\beta$  is a vector of parameters,  $x_i$  is the vector of predictors and  $\varepsilon$  is a normally distributed error (Salas et al., 1980).

Equation 1 can be rewritten in the following form (Fahrmeir and Tutz, 2001):

$$y_i \sim N(\mu_i, \sigma^2) \quad \eta_i = \alpha + \beta x_i \quad \eta_i = g(\mu_i) \quad i = 1, \dots, n \quad (2)$$

where,  $\mu_i$  is the expectation of  $y_i$ ,  $\eta_i$  is a linear predictor,  $g(\cdot)$  is the function that links the expectation of the response variable with the predictors (i.e. a link function). The link function is equal to the identity in the model described by Equation 1.

The model described by Equation 2 can be extended to a more general case (GLMs) with the assumption that each  $y_i$  has a distribution in the exponential family with expectation  $E(y_i/$

$x_i) = \mu_i$ , a common dispersion parameter  $\phi$  independent of  $i$  and function of the response variable variance (Fahrmeir and Tutz, 2001). The density function of these distributions is:

$$f(y_i|\theta_i, \phi) = \exp \left\{ \frac{y_i\theta_i - b(\theta_i)}{a(\phi)} + c(y_i, \phi) \right\} \quad (3)$$

where,  $\theta_i$  is the natural parameter (dependent on  $\mu_i$ ),  $a(\cdot)$ ,  $b(\cdot)$  and  $c(\cdot)$  are specific functions related to the type of exponential family.

The exponential family comprises some famous continuous (e.g. Normal, Lognormal and Gamma) and discrete (e.g. Poisson and Bernoulli) distributions and the link between its expectation and the linear predictors may be represented by any monotonic differentiable function (McCullagh and Nelder, 1989). Hence, the flexibility of GLMs to model different types of data (e.g. continuous, discrete and categorical) and Gaussian and non-Gaussian patterns.

Although the GLMs were proposed to model independent variables, they can be extended to time series with lags as covariates (Fahrmeir and Tutz, 2001; Chandler, 2005). A more detailed description of the GLMs theory is in McCullagh and Nelder (1989) and Fahrmeir and Tutz (2001).

### 3.2. Bivariate Copulas

Copulas are parametric functions that are able to combine marginal distributions into a multivariate distribution function. The copula concept allows flexibility to choose the univariate marginal distributions due to its dependence structure that sits within alternative variables that are uniform in the unit square and correspond to the values of the univariate cumulative distributions (Nelsen, 2007).

According to Sklar's theorem (Sklar, 1959), a bivariate distribution function  $F(x, y)$  of two correlated random variables  $X$  and  $Y$  with respective marginal cumulative distributions  $F(x)$  and  $F(y)$ , can be defined as a copula  $C$ :

$$F(x, y) = C(F(x), F(y)) = C(u, v) \quad (4)$$

where  $u$  and  $v$  are uniform and defined in the  $[0,1]$  interval and refer to the values of  $F(x)$  and  $F(y)$ , respectively.

Besides their marginal distribution flexibility, copulas can capture non-linear dependence features, their parameters can be estimated by maximum likelihood and there is a wide range of copula families (e.g. Normal, Frank, Gumbel, Clayton) which allows versatility in the dependence structure modelling as well. Some copula families' descriptions, their formulation and parameter estimation methods can be found in Joe (1997), Nelsen (2007) and Joe (2014).

There are copulas defined for more than two variables; however higher dimension copulas are simply one parameter constructs and result in loss of flexibility and rigid dependence assumptions. It is better to model the joint distributions as a sequence of bivariate copulas (i.e. the vine copula method). Some are applied to pairs of univariate margins and others applied to pairs of univariate conditional distributions (Aas et al. 2009; Joe, 2014). Still, the number of parameters grows exponentially with the number of variables in the vine copula approach. Fortunately, we are only dealing with a pair of time series.

### 3.3. GLM Single Site Streamflow Simulation

The annual streamflow time series for each site is modelled as a univariate GLM considering the annual streamflow lags with significant correlations (1<sup>st</sup>, 10<sup>th</sup>, 11<sup>th</sup>) as covariates (Figure 2). The inflows to JAG were sampled from a Lognormal distribution with identity link and those to MET, from a Gamma with log link (Figure 3). These models can be described as:

$$f(JAG_t) \sim \text{Lognormal}(\mu_{1,t}, \sigma_1^2): g(\mu_{1,t}) = \beta_{1,0} + \beta_{1,1}JAG_{t-1} + \beta_{1,2}JAG_{t-10} + \beta_{1,3}JAG_{t-11} \quad (5)$$

$$f(MET_t) \sim \text{Gamma}(\mu_{2,t}, \sigma_2^2): h(\mu_{2,t}) = \beta_{2,0} + \beta_{2,1}MET_{t-1} + \beta_{2,2}MET_{t-10} + \beta_{2,3}MET_{t-11} \quad (6)$$

where  $JAG_t$  and  $MET_t$  are each equivalent reservoir time series,  $t$  is the time,  $\mu_{1,t}$  and  $\mu_{2,t}$  are each series expected values for time  $t$ ,  $g(\cdot)$  and  $h(\cdot)$  are the link functions identity and log respectively,  $\sigma_1^2$  and  $\sigma_2^2$  are the series variance and  $\beta_{1,i}$  and  $\beta_{2,i}$  ( $i = 1, 2, \dots, \text{number of covariates} + 1$ ) are each series GLM parameters.

Due to the computer package support, the fitting of the Lognormal distribution to the JAG series occurred by applying the Gaussian distribution function to the logarithm of the data.

Maximum likelihood GLM parameter estimates are obtained using iterative weighted least squares (McCullagh and Nelder, 1989). This procedure was carried out using the ‘base’ stats package from the R programming language (R Core Team, 2013).

### 3.4. Copula GLM Multisite Streamflow Simulation

The joint distribution of both sites’ times series is modelled as a bivariate copula:

$$F(JAG_t \leq jag_t, MET_t \leq met_t) = C(F(JAG_t), F(MET_t)) = C(u, v) \quad (7)$$

This model assumes that the spatial relation between inflows to JAG and MET is temporally stationary. Also,  $u$  and  $v$ , the marginal’s CDFs values, are random variables uniformly distributed between zero and one.

To obtain the random values  $(u, v)$ , one of the variables may be sampled from the uniform distribution, while the other from the conditional bivariate copula distribution that can be defined as a function of the joint distribution:

$$F(v|u) = C(v|u) = \frac{\partial C(u, v)}{\partial u} \quad (8)$$

The selection of the copula family and parameters estimation was done with the ‘VineCopula’ R-package (Schepsmeier et al., 2018). The package estimates the parameters for different copula families, using the Maximum Likelihood method and then selects the family with the lowest Akaike Information Criterion (AIC); it also verifies the performance of the fit by the reproduction of the Kendall  $\tau$  correlation coefficient.

Also, a verification of the copula’s tail asymmetry is carried out with the lower ( $q_L$ ) and upper ( $q_U$ ) tail-weighted bivariate measures of dependence proposed by Krupskii and Joe (2015). The two measures are defined as:

$$q_L(a, p) = Cor \left[ a \left( 1 - \frac{u}{p} \right), a \left( 1 - \frac{v}{p} \right) \middle| u < p, v < p \right] \quad (9)$$



$$Q_U(a, p) = Cor \left[ a \left( 1 - \frac{1-u}{p} \right), a \left( 1 - \frac{1-v}{p} \right) \middle| 1-u < p, 1-v < p \right] \quad (10)$$

Where  $a(\cdot)$  is a monotonic increasing function in the  $[0,1]$  domain and  $p$  is the truncation level with values in the  $(0,0.5]$  interval. The monotonic increasing function and truncation level used were respectively  $a(x) = x^6$  and  $p = 0.5$  as recommended by Krupskii and Joe (2015).

Equations 7 and 8 provide only the spatial correlation structure. The temporal dependence is modelled, within each series marginal distribution, as the single site GLMs described by Equations 5 and 6. Thus, after  $u_t$  and  $v_t$  (spatially correlated variables) are sampled,  $JAG'_t$  and  $MET'_t$  (temporally and spatially correlated variables) can be determined by the inverse of the respective GLM's CDF.

### 3.5. Generation Algorithm

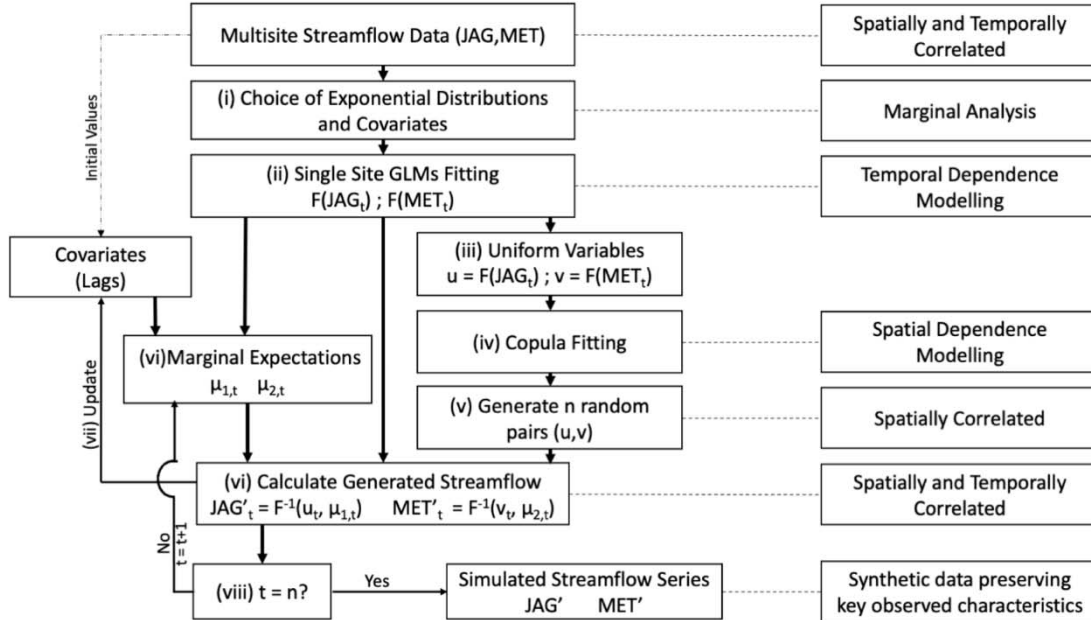
The proposed multivariate annual streamflow simulation procedure is detailed in Figure 4. It can be described as an eight-step process:

- i. The probability distributions of the annual inflow series at the equivalent reservoirs are evaluated to select the respective best fit exponential functions and the lags with relevant correlation coefficients that should compose the covariates.
- ii. The temporal dependence is modelled as described by Equations 5 and 6 by fitting univariate GLMs with the covariates and exponential distributions selected for each series (marginal distributions) in step i.
- iii. The uniform u-v variables are calculated from the estimated expectations and the GLMs' CDFs at each time position.
- iv. The spatial correlation structure is established by fitting a copula distribution between the observed u-v uniform variables.
- v. After modelling both dependence structures, the random simulation starts with the generation of  $n$  (the length of the synthetic time series) random  $u$  from the

uniform  $[0,1]$  distribution and then  $n$  random  $v$  are drawn from the bivariate copula conditional distribution (Equation 8).

- vi. The first ( $t = 1$ ) synthetic generated  $u_t$ - $v_t$  pair (spatially correlated) is transformed into the  $JAG'_t$  and  $MET'_t$  synthetic streamflow pair (temporally and spatially correlated) by the inverse of the marginals GLMs' CDF with expectations determined from the set of covariates (lags) values (the initial set may be a random sample from the historical series).
- vii. The set of covariates values is updated with the generated  $JAG'_t$  and  $MET'_t$ .
- viii. The time position is updated ( $t = t+1$ ) and the steps vi and vii are repeated for the next  $u_t$ - $v_t$  pairs until all pairs are transformed into the synthetic generated streamflow series ( $t = n$ ).

Figure 4 – Flowchart of the GLM-Copula annual streamflow generation procedure.



### 3.6. Performance Assessment

In order to demonstrate the performance of the single site GLM and of the multisite GLM Copula annual streamflow time series stochastic simulation models, their efficiency is compared respectively to univariate autoregressive (AR) and multivariate ARMA models

described by Salas et al. (1980). The multisite GLM Copula is also compared to the state-of-art copula model, COPAR. The synthetic replicates from the stochastic models should preserve the statistical characteristics (i.e. mean, standard deviation and skewness) and the dependence structures (Srivastav and Simonovic, 2014).

The univariate AR and the multivariate ARMA models were fitted to the normalized JAG and MET inflow series. The data normalization was done using the Box-Cox power transformation. The fitting and sampling procedures were carried out with the R MARIMA package (Spliid, 2017). The first order univariate AR and the (1,1) order multivariate ARMA were selected since they resulted in the lowest AIC values, as shown in Table 1.

Table 1 - AIC values for all the AR/ARMA models tested.

Model	AIC	
	JAG	MET
AR(1)	-5765	-6431
AR(2)	-5123	-6139
AR(3)	-5065	-5841
ARMA(1,1)	-9832	
ARMA(1,2)	-8850	
ARMA(2,1)	-8674	
ARMA(2,2)	-8333	

The COPAR model (Brechmann and Czado, 2015) applies the Vine Copula theory (Aas et al., 2009) to model both serial and cross-sectional dependences. Vine copulas are based on the decomposition of the multivariate copula density into a product of bivariate copulas, also called pair copula construction.

In this paper, a first order COPAR (1) model is chosen as benchmark. It was reproduced through the original algorithm described in Brechmann and Czado (2015). The application of the COPAR (1) to the case study time series required the sequential fitting of five bivariate copulas:  $C(JAG_t, JAG_{t-1})$ ,  $C(JAG_t, MET_t)$ ,  $C(JAG_{t-1}, MET_t / JAG_t)$ ,  $C(MET_{t-1}, JAG_t / JAG_{t-1})$  and  $C(MET_{t-1}, MET_t / JAG_{t-1}, JAG_t)$ .

The families and parameters of each of the bivariate copulas were estimated using the Two-Stage Maximum Likelihood Estimation method where the parameters of marginal distributions are initially estimated and then the parameters of the copula function are estimated using Maximum Likelihood with the marginals computed from the previously fitted marginal distributions (Singh and Zhang, 2018). The fitting and simulation procedures of the COPAR model were carried out with functions from the ‘VineCopula’ R-package.

One hundred synthetic annual streamflow series (runs) with the same length as the observed series ( $n = 101$  years) are generated by each model and their statistical characteristics and dependence structures are compared graphically based on boxplots against the historical data. A historical series behavior is judged to be preserved by the synthetic series when its values lie within the box (Salas and Lee, 2010; Lee and Salas, 2011; Hao and Singh, 2013). The use of one hundred runs is in accordance with the streamflow simulation literature (Lee and Salas, 2011; Hao and Singh, 2013; Srivastav and Simonovic, 2014).

As a nonlinear measure of performance, the copula entropy (CE) of the observed variables ( $JAG_t, JAG_{t-1}, MET_t, MET_{t-1}$ ) was compared to the CE of the model’s synthetic series. Based on the definition of Shannon’s Entropy (Shannon, 1948), Ma and Sun (2011) proposed the copula entropy as the entropy of the copula function and showed its relation with joint and marginal entropy. They also proved the equivalence between the negative of CE and mutual information (MI).

MI is a traditional non-linear measure of the dependences/association between random variables based on entropy theory (Cover and Thomas, 1991). However, the estimation of MI for more than two variables is a hard task, while CE just requires the variables copula joint distribution (Alpettiyil Krishnankutty et al., 2020). Thus, CE is a useful multivariate estimator of MI.

CE has been used to measure the association between stock market variables (Zhao and Lin, 2011), multiple degradation processes (Sun et al., 2019) and river flows (Chen et al., 2013a). It was also used as a performance measure in feature selection for rainfall-runoff modeling and drought prediction (Chen et al., 2014; Huang and Zhang, 2018) and in selecting vine copula structure for multisite streamflow simulation (Ni et al., 2020).

In this research, the copula entropy of the observed data and the resulted from the synthetic time series were calculated through the ‘copent’ R package (Ma, 2020) which calculates CE through a nonparametric estimation of the copula function.

As a practical exercise, we also analyzed the performance of the models to simulate drought conditions, simply understood as being below average conditions. For this purpose, in each case study, the years with annual flows below the respective historical mean were assigned to drought conditions.

The maximum number of consecutive years under drought conditions (i.e. the longest drought period) in each of the one hundred synthetic series of the GLM-Copula, ARMA and COPAR models were compared to the longest drought period of the historical series. The longest period under drought conditions is a relevant constraint in the design and in the operation of the artificial reservoirs.

## **4. RESULTS**

### **4.1. GLM Single Site Streamflow Simulation**

The ability of the single site GLM and AR methods to preserve the historical statistics and temporal dependence structures is presented respectively in Figures 5 and 6. For this purpose and like all the other figures, boxplots were drawn of the generated values of the annual statistics and these were compared with the historical statistics. For the boxplots, the whiskers have maximum length of  $1.5 \times \text{IQR}$  (interquartile range) and the values outside the whiskers are considered to be outliers (Robbins, 2012).

Figure 5 shows that all the historical statistics are well reproduced by both methods except for the standard deviation of the inflows to MET from the GLM model and for the minimum of the inflows to JAG from the AR model. Individually, the GLM reproduced better the minimum and the skewness coefficient, the first since the AR model underestimated the minimum of both series and the latter may be due to not requiring data normalization. Also, the methods were better in reproducing the maxima than the minima and, overall, presented the same performance in both JAG and MET regarding the replication of the sample statistics.

From the autocorrelation function (ACF) analysis in Figure 6, both methods were similarly efficient in representing the first lag autocorrelation (the short-term temporal dependence) and also had similar dispersions. The GLM also depicted the long-term dependence peak at the 10<sup>th</sup> and 11<sup>th</sup> lags, however with better performance for the MET inflow series (gamma distribution). An interesting advantage presented by the GLM series is that their ACF is not represented as an exponential decay like the autoregressive models but instead it is able to capture the lagged correlations used as covariates (1<sup>st</sup>, 10<sup>th</sup> and 11<sup>th</sup>). Thus, the GLM can be applied to mimic some complex ACF designs by considering a larger set of lags as covariates. However, the increase of the set of covariates increases the number of parameters and reduces the parsimony of the model which can be a drawback depending on the ratio between the length of the observed series and the number of parameters.

Figure 5 – Comparison, for both equivalent reservoirs (JAG and MET), of some of the annual statistics of the historical series and of the synthetic series obtained by the GLM and AR models. The box ranges from the first to the third quartile and the whiskers have maximum length of  $1.5 \times \text{IQR}$  (interquartile range).

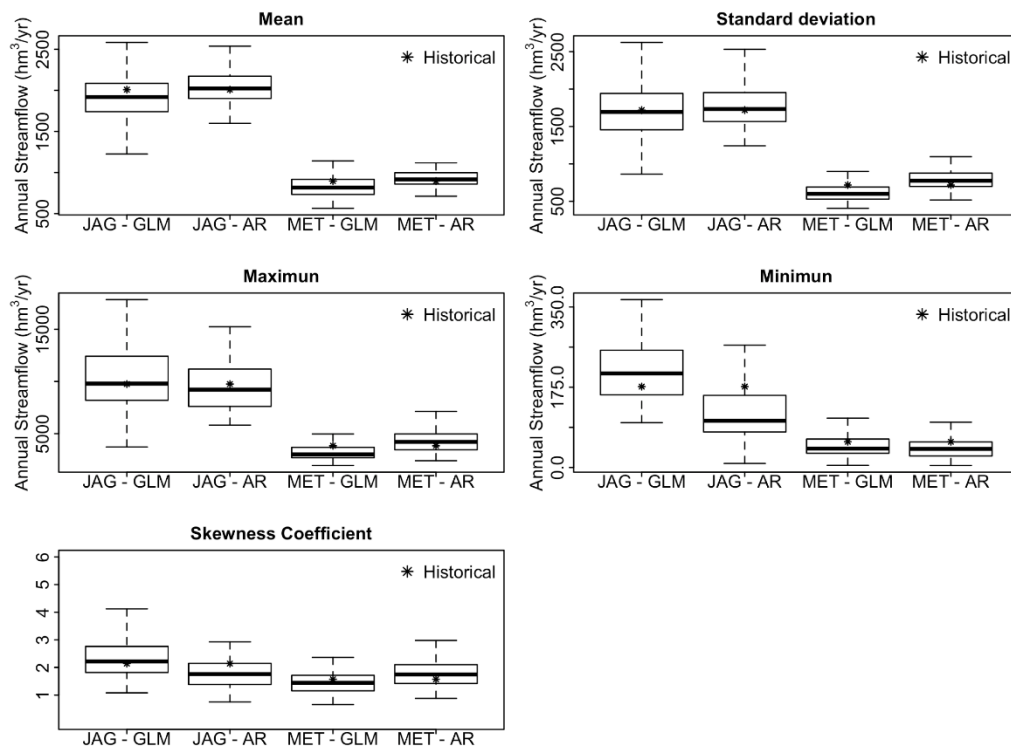
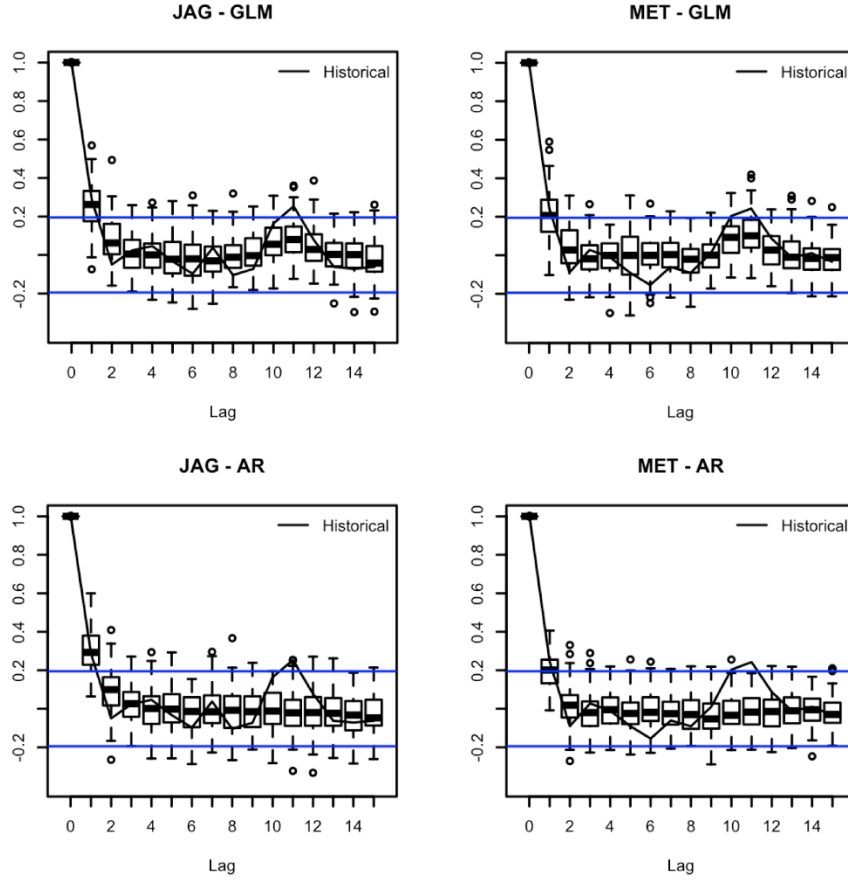


Figure 6 – Comparison, for both equivalent reservoirs (JAG and MET) of the annual autocorrelation function of the historical series and of the univariate synthetic series obtained by the GLM (top) and AR (bottom) models. The boxes range from the first to the third quartile and the whiskers have maximum length of  $1.5 \times \text{IQR}$  (interquartile range).



## 4.2. GLM Copula Multisite Streamflow Simulation

### 4.2.1. Copula Fitting and Family Selection

Table 1 presents the estimated parameters, the tail-weighted dependence metrics ( $\rho_L$ ,  $\rho_U$ ) and the performance metrics of different copula families to model the joint distribution of the annual inflows at JAG and MET equivalent reservoirs. The Kendall  $\tau$  is a nonlinear measure of correlation between two series.

The copula family defines how the joint distribution is modeled. For instance, the Gaussian copula represents the joint distribution with the same association intensity despite the values, while the Gumbel copula has a higher association for large values and the Clayton copula for lower values. The Frank copula has a high association for the middle values and low in the extremes (Lee and Salas, 2008). More details of the tested copula families can be found in Nelsen (2007) and Joe (2014).



Copula tail asymmetry can be inferred from the  $\varrho_L$  and  $\varrho_U$  values: i) if  $\varrho_L$  is stronger than  $\varrho_U$  then the joint probability distribution might have greater values in the joint lower tail, i.e. there is tail asymmetry toward the joint lower tail; ii) if  $\varrho_L$  is weaker than  $\varrho_U$  then the joint probability distribution might have greater values in the joint upper tail, i.e. there is tail asymmetry toward the joint upper tail; iii) if  $\varrho_L$  is about equal  $\varrho_U$  then the joint probability distribution values in both tails might be similar, i.e. there is no tail asymmetry. With these definitions, it is possible to understand the tail asymmetry of the observed data and of each of the fitted copulas presented in the Table 1.

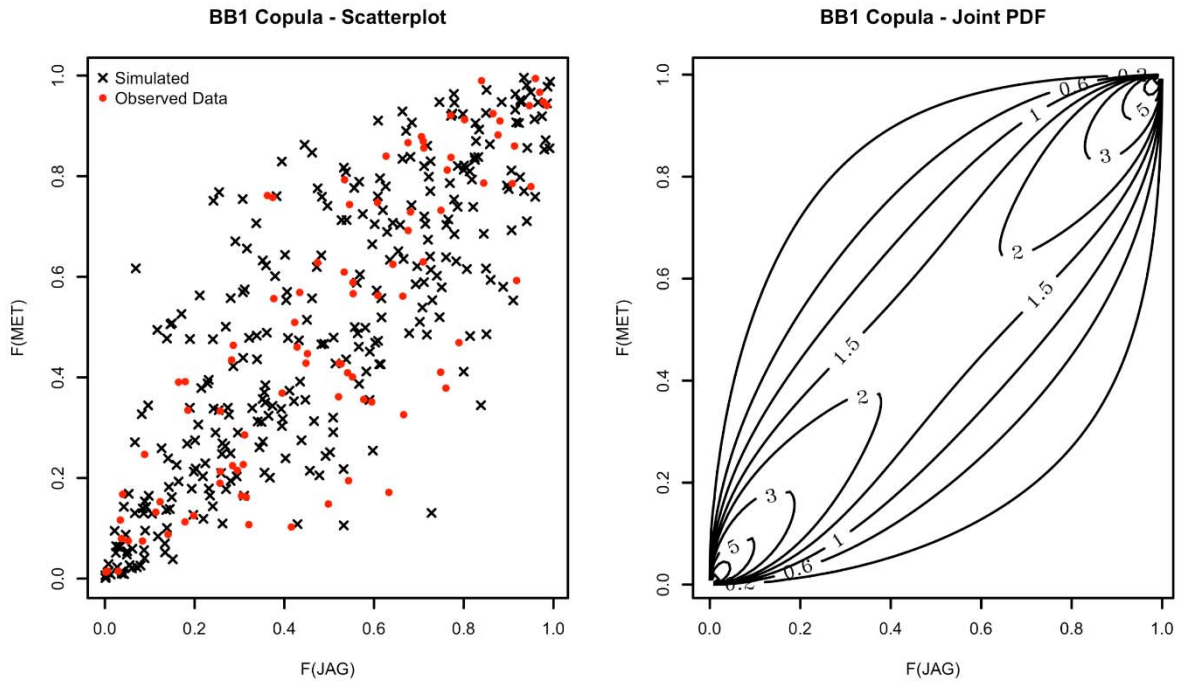
The Gaussian and Student copulas presented the minima AIC values and the Kendall  $\tau$  values closest to the observed. However, as the observed data presented a small tail asymmetry towards the lower joint tail, symmetrical copulas like the Gaussian and Student  $t$  copulas might not be the best suited to model the observed data. Therefore, the BB1 copula, which is the fitted copula with asymmetry towards the lower tail that presented the lowest AIC value, was the copula selected to model the spatial dependence for the case study.

Figure 7 illustrates the scatterplot of 300 random uniform pairs (F(JAG), F(MET)) simulated from the BB1 copula versus the observed values. It also depicts the contour plot of the BB1 copula joint probability distribution values. Figure 7 shows that dependence structure was well preserved by the BB1 copula.

Copula	Parameters Names	Parameters Values	Kendall $\tau$	$\varrho_L$	$\varrho_U$
Observed Data	-	-	0.67	0.81	0.64
Gaussian	$\rho$	0.85	0.65	0.67	0.67
Student t	$\rho; \nu$	0.85; 30	0.64	0.68	0.68
BB1	$\theta; \delta$	0.73; 1.93	0.62	0.76	0.65
Rotated Gumbel (180°)	$\delta$	2.6	0.62	0.81	0.50
Frank	$\delta$	8.95	0.64	0.41	0.50
Gumbel	$\delta$	2.52	0.60	0.47	0.76
Clayton	$\delta$	2.31	0.54	0.84	0.17
Joe	$\delta$	2.87	0.50	0.10	0.78

Table 1 – Copula families applied to model the joint distribution of the annual flows at the JAG and MET equivalent reservoirs. Estimated parameters, tail-weighted dependence metrics and fit performance. Ordered from lowest to highest AIC values. Note that the BB1 copula is the one, with asymmetry towards the lower tail ( $\varrho_L > \varrho_U$ ), that is closest to the observed data.

Figure 7 – BB1 copula simulation versus observed data scatterplots (left) and BB1 copula joint probability distribution function contour plot (right). Both plots are in the  $[0,1]$  uniform space.

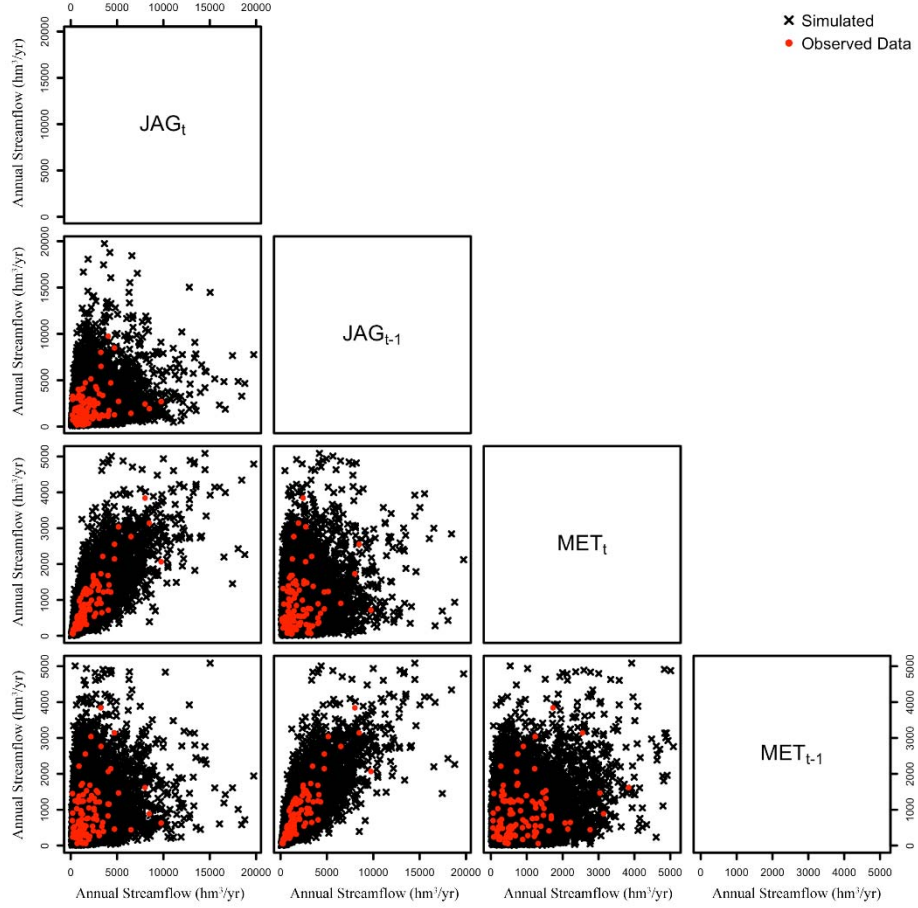


#### 4.2.2. Preservation of the dependency structure and historical statistics

Figure 8 presents, as an illustration of the dependency structure, the pair plot of the  $JAG_t, JAG_{t-1}, MET_t, MET_{t-1}$  variables for the observed data and for the synthetic series generated by the GLM-Copula model. The GLM-Copula model visually reproduced the dependency structure of the observed variables.

Figure 8 – Temporal and spatial dependency structures scatterplot, 100 points of observed data (red circles) and 10000 points of simulated data (black crosses) from the GLM-

Copula multivariate model. The panels in the off-diagonal show the relationships between the classifications on the diagonal blocks.



For both equivalent reservoirs, Figures 9, 10 and 11 compare some statistical characteristics of the historical series with those related to the dependence structure of the synthetic annual flow series generated by the GLM-Copula, ARMA and COPAR multivariate models.

All three methods were able to reproduce the historical statistics with similar efficiency. Like the univariate case, the GLM based model carried out the skewness coefficient better than ARMA and the ARMA model underestimated the minimum values.

From the auto and cross-correlation functions, Figures 10, 11 and 12 for the GLM-Copula, ARMA and COPAR models respectively, the methods represented the short-term

dependence structure, i.e. the first lag autocorrelation (temporal dependence) and the lag 0 cross-correlation (spatial dependence), with matched efficiency and spreads.

Like the univariate GLM model, the GLM-Copula model also has the ability to represent the long terms dependencies as its correlation function do not necessarily follow an exponential decay (Figure 10), which is not the case of the ARMA model regarding the long-term dependencies (Figure 11). Thus, the proposed model showed the same performance in representing the short-term dependencies than the ARMA and COPAR models, while having the advantage over ARMA of being flexible and intuitive to depict isolated peaks in the auto and cross-correlation functions by choosing the appropriate lags as covariates and being simpler than the COPAR model.

Figure 9 – Comparison, for both equivalent reservoirs (JAG and MET), of some of the annual statistics of the historical series and of the synthetic series obtained by the multivariate GLM-Copula, ARMA and COPAR models. The boxes range from the first to the third quartile and the whiskers have maximum length of  $1.5 \times \text{IQR}$  (interquartile range).

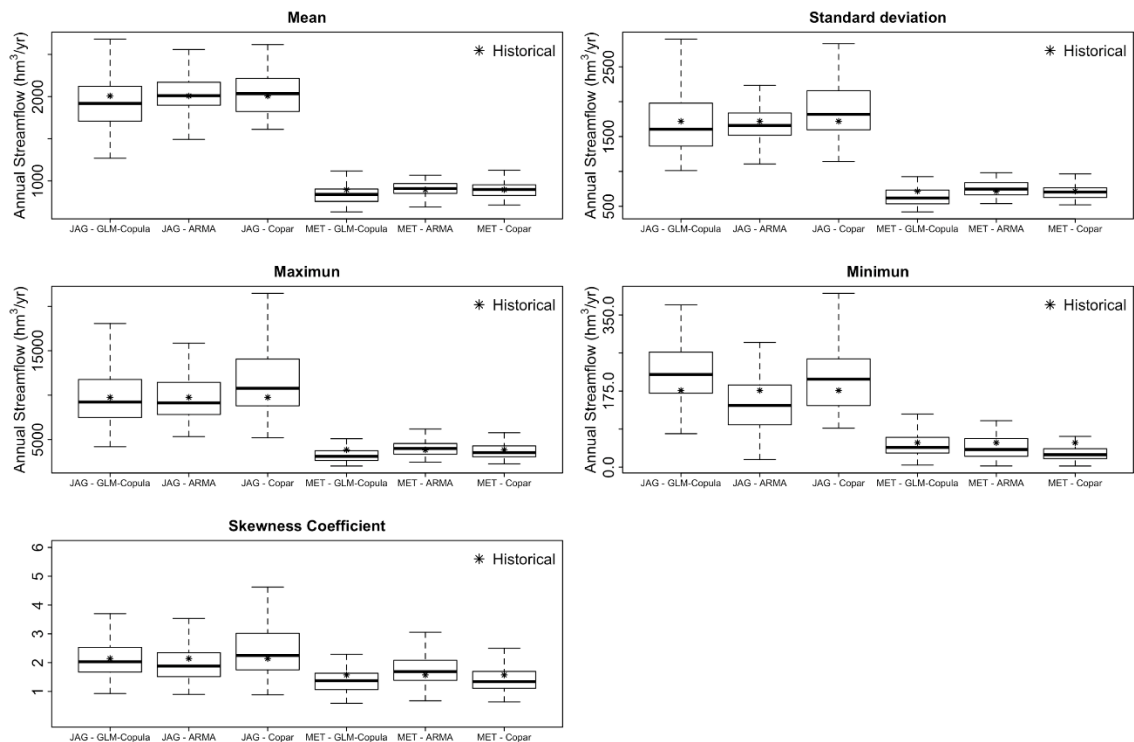


Figure 10 – Comparison, for both equivalent reservoirs (JAG and MET) of the annual auto and cross-correlation functions of the historical series and of the multivariate synthetic series obtained by the GLM-Copula model. The boxes range from the first to the third quartile and the whiskers have maximum length of  $1.5 \times \text{IQR}$  (interquartile range).

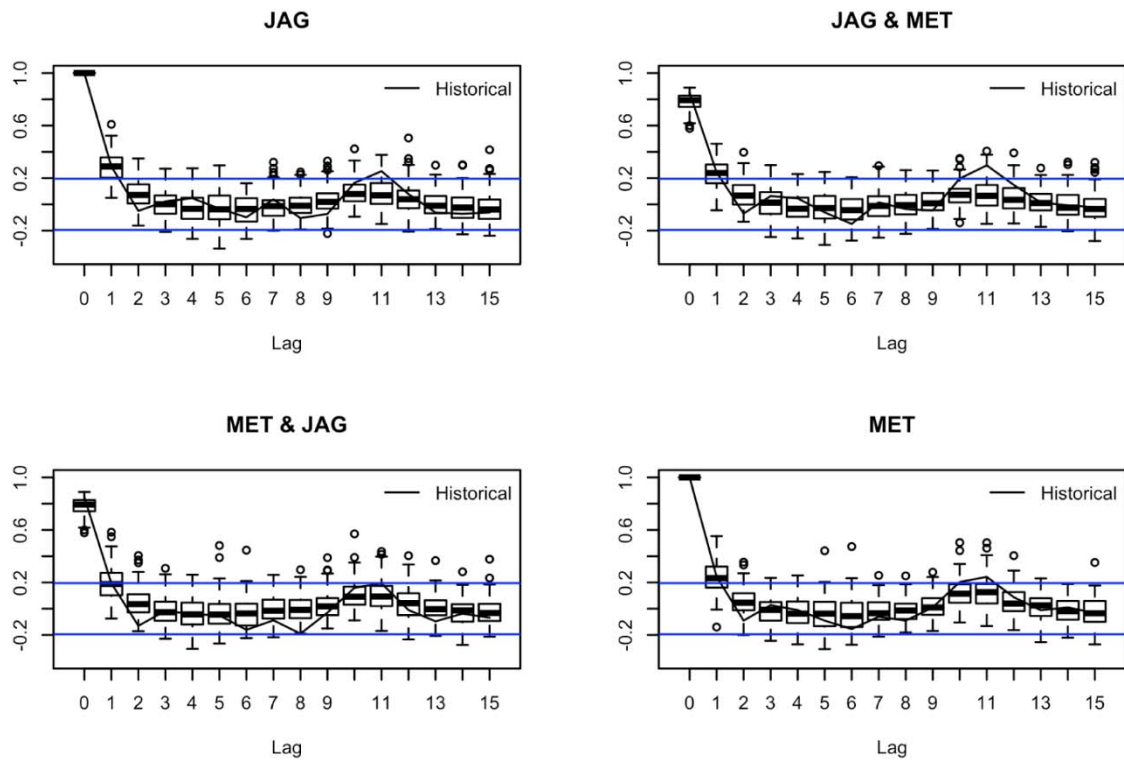


Figure 11 – Comparison, for both equivalent reservoirs (JAG and MET) of the annual auto and cross-correlation functions of the historical series and of the multivariate synthetic series obtained by the ARMA model. The boxes range from the first to the third quartile and the whiskers have maximum length of  $1.5 \times \text{IQR}$  (interquartile range).

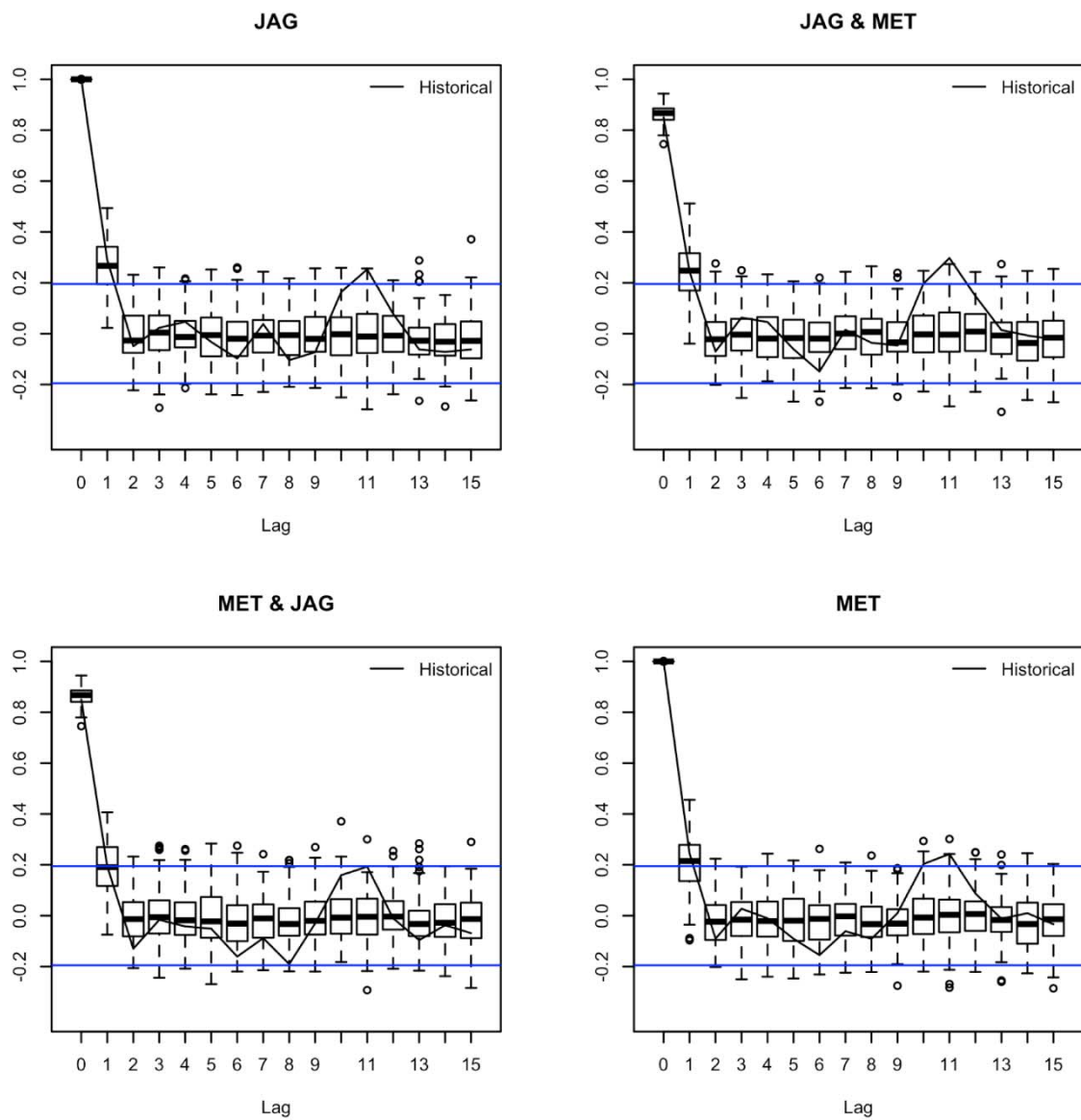
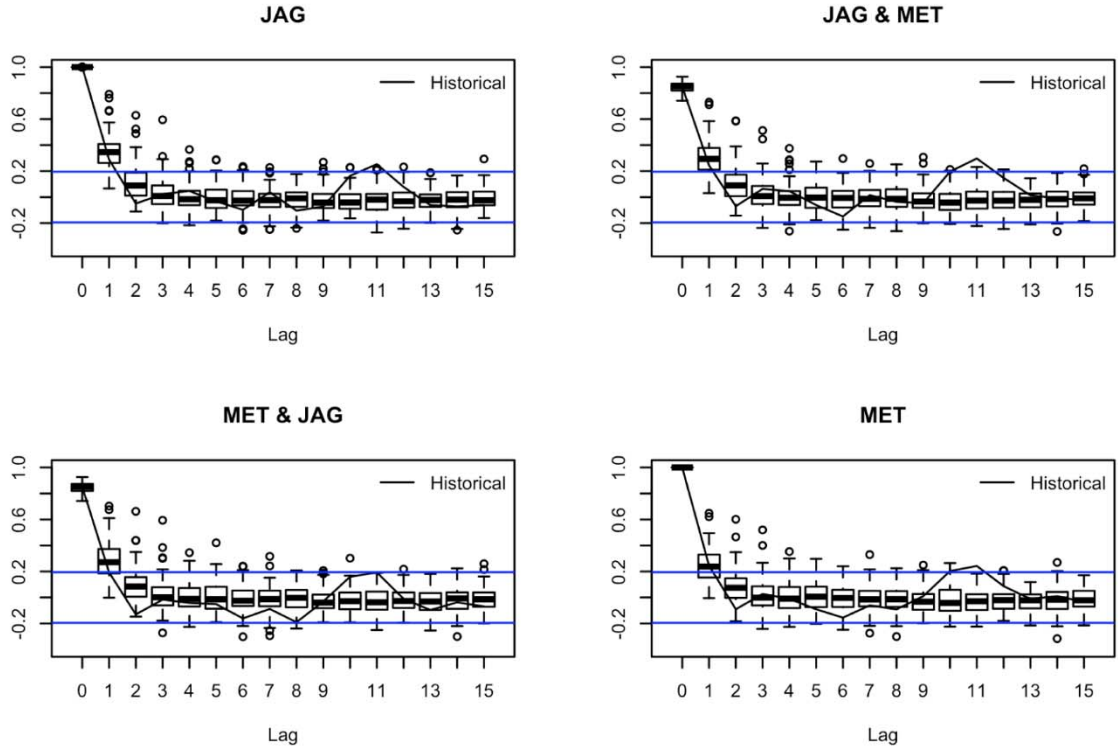


Figure 12 – Comparison, for both equivalent reservoirs (JAG and MET) of the annual auto and cross-correlation functions of the historical series and of the multivariate synthetic series obtained by the COPAR model. The boxes range from the first to the third quartile and the whiskers have maximum length of  $1.5 \times \text{IQR}$  (interquartile range).



The relative errors (Equation 11) of the statistical characteristics between the synthetic and the historical series were computed as another performance measure (Silva and Portela, 2012) and are presented in Table 2.

*Relative error (%)*

$$= \frac{Gen - Hist}{Hist} \times 100 \quad (11)$$

where Gen denotes the mean of the 100 statistics estimated from the generated synthetic series and Hist the same statistic estimated from the corresponding historical sample.

The results of Table 2 corroborate those denoted by the previous boxplots and are not conclusive as to whether there is a better model for simulating annual streamflow when comparing the preservation of historical statistics. However, it can be noticed that GLM-Copula was the best in reproducing the temporal dependence statistic for both series which is likely to be due to the GLM's margin modeling. In contrast, the GLM-Copula was the worst in reproducing the spatial dependence statistics.

In comparison to the ARMA model, the GLM-Copula reproduced the Skewness better for both series while being worse reproducing the mean. By comparing GLM-Copula and COPAR, it can be noticed that the former was better in reproducing JAG statistics while the latter was better in reproducing MET's, which also happened in the comparison between ARMA and COPAR.

Statistics	JAG – Relative error %			MET – Relative error %			Historical values	
	GLM-Copula	ARMA	COPAR	GLM-Copula	ARMA	COPAR	JAG	MET
Mean	-4.09	<b>1.01</b>	2.71	-6.03	1.18	<b>0.80</b>	2007.91	896.24
Standard deviation	<b>-1.35</b>	-1.42	14.31	-10.42	5.63	<b>-0.17</b>	1719.42	717.27
Maximum	2.02	<b>1.20</b>	25.89	-14.79	10.15	<b>-2.59</b>	9751.80	3841.52
Minimum	24.25	-15.71	<b>12.49</b>	<b>-3.8</b>	-17.66	-38.92	176.38	56.13
Skewness	<b>2.08</b>	-6.84	16.94	-11.86	16.30	<b>-7.31</b>	2.11	1.55
Lag-1 auto-correlation	<b>-1.59</b>	-8.73	18.46	<b>-1.74</b>	-14.07	2.54	0.29	0.24
Lag-0 cross-correlation	-8.32	1.76	<b>-0.57</b>	-			0.85	

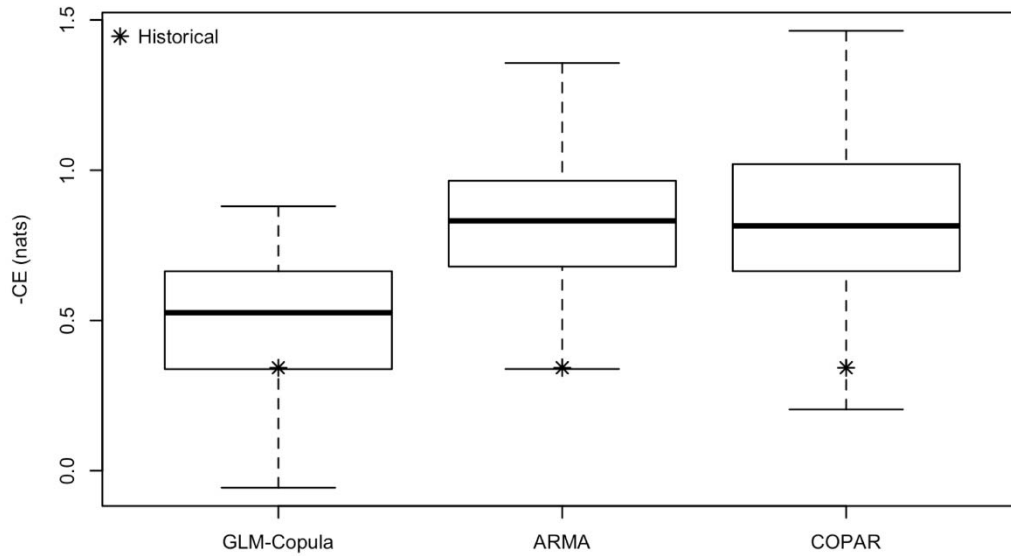
Table 2 – Relative errors of the annual parameters and historical values for both equivalent

reservoirs. The values in **bold** identify the criterion with the best performance.

Figure 13 presents the comparison of the copula entropy for the original data and the models' synthetic series as a nonlinear measure of total association between the variables ( $JAG_t$ ,  $JAG_{t-1}$ ,  $MET_t$ ,  $MET_{t-1}$ ). It shows that the three models resulted in higher association than the observed data and that the GLM-Copula model was the closest to the observed total association and reasonable better than both benchmark models.

Figure 13 – Comparison of the copula entropy (CE) for the observed data and the synthetic series obtained by the multivariate GLM-Copula, ARMA and COPAR models. The boxes range from the first to the third quartile and the whiskers have maximum length of 1.5 x IQR (interquartile range).



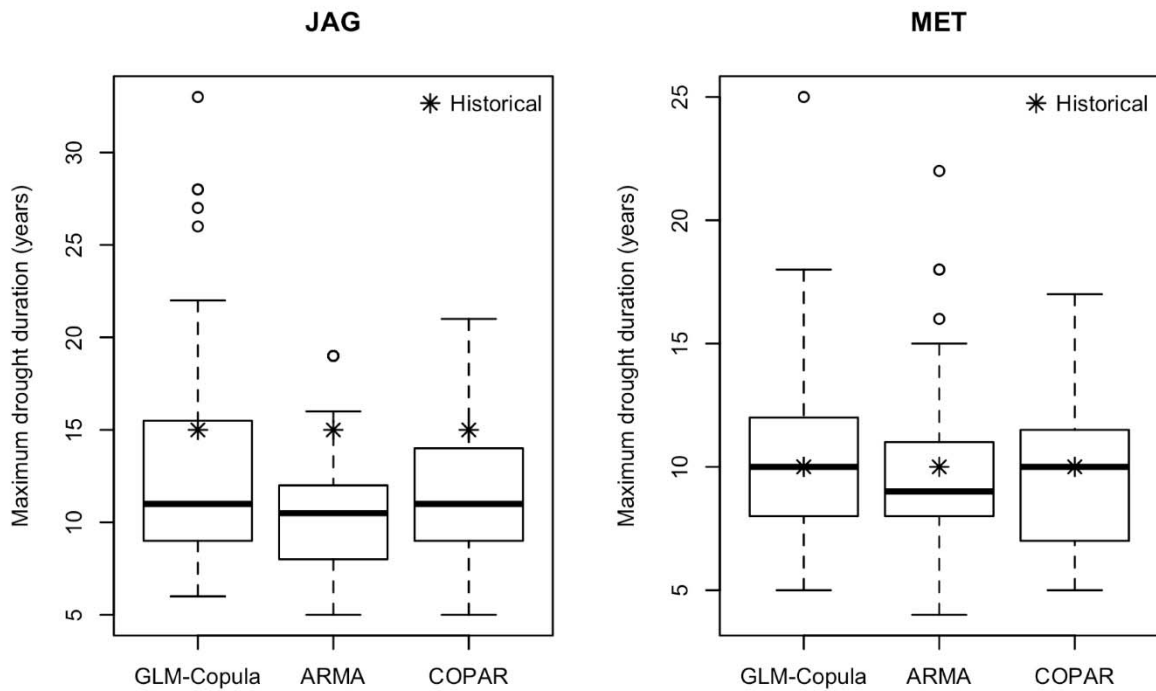


#### 4.2.3. Drought conditions

In Figure 14, the longest drought period from each of the synthetic series are compared with the historical values. Although the methods applied matched performance in reproducing the historical statistics, the GLM-Copula model was significantly superior in simulating drought duration for the JAG inflow series, however with greater spreads. The ARMA longest drought showed lower durations than the GLM-Copula's and led to an underestimation in the JAG series. Both copula models (GLM-Copula and COPAR) were better than ARMA in this criterion for both series. For MET, the GLM-Copula and the COPAR presented matched performance while ARMA was slightly worse.

While the greater dispersion presented by the GLM-Copula and COPAR time series models would not be a problem in the stochastic optimization of the reservoir system operation rules, the use of the ARMA generated series would imply a false higher water availability for the JAG series, increasing the vulnerability of the system to longer droughts and the risk of water shortage due to the pluriannual characteristic of the reservoirs.

Figure 14— Maximum drought duration comparison for both equivalent reservoirs (JAG and MET) of the historical and of the multivariate synthetic time series generated by the GLM-Copula, ARMA and COPAR models. The boxes range from the first to the third quartile and the whiskers have maximum length of  $1.5 \times \text{IQR}$  (interquartile range).



## 5. SUMMARY AND CONCLUSIONS

This paper presents the implementation of a new multisite stochastic annual streamflow simulation approach based on the combination of bivariate copulas (spatial dependence) and Generalized Linear Models (temporal dependence). This research also brought a simple application of GLM to generate univariate streamflow time series. The authors believe this work is the first research to apply Generalized Linear Models to stochastic streamflow simulation.

The GLM-Copula time series model efficiently exploits synergies and the flexibility of both techniques and its main advantages are that they:

- i. Do not require data normalization, hence the GLMs flexibility to deal with any exponential family distribution.

- ii. Have capacity to represent non-conventional long-term ACF designs intuitively by just considering significant lags as covariates of the GLMs.
- iii. And have flexibility to model spatial dependence by defining the copula family

The results showed that the GLM-Copula approach ability to preserve summary statistics from the historical data was similar to the classical multivariate ARMA and the state-of-art COPAR models. For the dependency structures, the GLM-Copula reproduced what was narrowly the best in reproducing the short-term temporal dependence (lag-1 autocorrelation), narrowly the worst in reproducing the spatial dependence (lag-0 cross-correlation) and reasonable the best in reproducing the total association (copula entropy). Thus, the proposed GLM-Copula model can be an alternative with matched, if not better, performance when compared to the existing time series simulation methods.

In comparison with the ARMA model, the GLM-Copula was better in reproducing both the skewness coefficient and the maximum drought duration, and the latter was underestimated by the ARMA model. COPAR was also better reproducing the maximum drought duration than the ARMA model.

These results are similar to those obtained by other copula approach studies of skewness coefficient replication (Lee and Salas, 2011; Chen et al., 2019;) and for drought representation (Lee and Salas, 2011). Although Lee and Salas (2011) considered these results as “marginal benefits”, we suggest that in both works it is clear that the ARMA models lead to an underestimation of drought conditions while the copula-based models do not. For an underdeveloped semiarid region like that considered in the case study, water resources planning with misleading drought information could result in heavy economical losses. Thus, the copula based GLM-Copula and COPAR synthetic series are preferable to those resulting from the ARMA model in drought dependent stochastic applications. In addition, the better reproduction of the skewness coefficient might be related to the lack of data normalization. Thus, GLM or

copula based methods like the GLM-Copula are flexible parametric approaches that can be applied even when data normalization fails.

Compared to the COPAR model, the GLM-Copula has the advantages of being simpler and reducing the computational burden for multisite and/or greater-than-one lag applications, while maintaining the flexibility of the marginal distributions modeling. The main drawback is that it does not model the temporal dependence nonlinearly.

Despite the existence of multiple time series simulation methods, this research showed that there is still space for improvement. The proposed method is intuitive, robust, requires low computational effort and can be easily replicated with open-source R packages. Therefore, the authors consider that the proposed model might be useful in future studies/applications due to its flexibility and the solid results presented.

The model was created in its simplest form and due to its flexibility, can be easily extended by combining Generalized Linear Models with numerical data or by extending them to include exogenous climate variables that affect streamflow. The extension of the GLM-Copula to higher dimensions (more than two spatially dependent time series) is straightforward by combining GLMs for temporal dependence modeling with vine or maximum entropy copulas for spatial dependence modeling. Modeling temporal dependencies in combination with GLMs would soften the curse of dimensionality in vine and maximum entropy copulas applications.

### **3 DYNAMIC MONTHLY STREAMFLOW FORECASTING. THE BRAZILIAN HIDROELETRIC SECTOR CASE STUDY**

#### **1. INTRODUCTION**

Streamflow forecasts are of great value to a wide range of stakeholders who are impacted by the unpredictable nature of the climate and would benefit from better understanding of climate variability and management of its related risks (Boucher et al., 2012; Matte et al., 2017; Cassagnole et al., 2021). This includes operators of hydroelectric power plants, who rely heavily on seasonal flow forecasts to anticipate water availability and to optimize accordingly energy production to achieve maximum reliability and minimum cost (Cassagnole et al., 2021).

The Brazilian National Electric System Operator (ONS) uses monthly streamflow forecasts as an integral part of its planning and operation of the electric system in Brazil. These forecasts are crucial to ensure a reliable supply of electric power throughout the year. The monthly streamflow are used by ONS for:

i) Operational Scheduling: Based on monthly flow forecasts, ONS can schedule the operation of hydroelectric plants. This includes deciding when to store water in reservoirs (during periods of higher flow) and when to release water for power generation (during periods of lower flow).

ii) Resource Planning: ONS uses the forecasts to plan the allocation of energy resources throughout the year. This includes deciding how much energy will be generated by hydroelectric, thermal, wind, and solar sources based on expected reservoir conditions.

iii) Generation Dispatch Signals: With monthly flow forecasts, ONS can issue generation dispatch signals to the power plants, indicating how much electric power should be generated in a particular month.

iv) Maintenance Planning: ONS uses flow forecasts to plan maintenance for hydroelectric plants, scheduling maintenance downtime during periods of higher flow when energy demand can be met by other sources.

v) Energy Trading: Flow forecasts are also used in the energy market for negotiations of electric power purchase and sale contracts since they affect prices and the availability of energy in the market.

There are two major approaches for streamflow forecasting: statistical and dynamical. The statistical approach is based on statistical regression techniques that can be enhanced with exogenous variables like predictors of sea surface temperature (Souza Filho and Lall, 2003; Souza Filho and Lall, 2004; Sankarasubramanian et al., 2009; Lima and Lall, 2010; Panahi et al., 2021; Porto et al., 2021). In the dynamical approach, climate and hydrological process are coupled by the forcing of hydrological models with numerical predictions from Atmospheric General Circulation Models (GCMs) (Block et al., 2009; Kwon et al., 2012; Ávila et al., 2023; Greuell and Hutjes, 2023). While the statistical approach is efficient as it is simpler and has lower computational requirements, the dynamical approach offers the benefit of integrating climate prediction and its efficacy improves with advancements in our comprehension of climate processes and the development of atmospheric modeling (Block et al., 2009).

The Brazilian electricity sector, one of the largest in the world with a total installed capacity of over 180 GW. The sector relies heavily on hydropower, which contributes to over 59% of the country's total installed capacity. Despite the recent growth of alternative sources such as wind and solar energy, hydropower remains a critical energy source. Water availability fluctuations caused by climate variability pose a significant vulnerability to the system, and drought periods are correlated with a decline in the GDP growth (Prado Jr. et al., 2016). This vulnerability underscores the importance and visibility of streamflow forecasting models in Brazil.

The Brazilian electricity sector currently relies predominantly on statistical models for streamflow forecasting, as evidenced by previous studies. The PREVIVAZ model, a well-known statistical approach, is widely used by the sector's operator (ONS, 2012). However, there is a noticeable lack of research on dynamic streamflow forecasting models at the national level. While some dynamic streamflow forecasting studies have been conducted at the catchment scale (Fan et al., 2016; Ávila et al., 2023), national-level investigations are scarce. This may be attributed to the satisfactory performance of statistical models and to criticisms that have arisen in the last decade regarding the limited ability of GCMs to forecast short-term rainfall patterns (Lima and Lall, 2010).

However, recent advances in our understanding and forecasting of climate have resulted in skillful and useful meteorological predictions, which can consequently increase the confidence of hydrological predictions. Two of these advancements were the improvement of seasonal forecasting models like the North American Multimodel Ensemble (NMME) (Becker et al., 2020; Becker et al., 2022) and of subseasonal forecasting models including the development of the NOAA/Climate Testbed Subseasonal Experiment Subseasonal Experiment (SubX) (Pegion et al., 2019).

SubX comprises an ensemble of subseasonal climate predictions from the North American models. The experiment has demonstrated skill in simulating the Madden-Julian Oscillation (MJO) and the North Atlantic Oscillation (NAO) (Pegion et al., 2019; Jiang et al., 2020; Feng et al., 2021), which are major sources of subseasonal predictability. Furthermore, these models have exhibited skillful predictions of temperature variability and precipitation up to three weeks ahead of time, although there is a strong regional variation of its performance with higher performances for the northern hemisphere and lower latitudes in the southern hemisphere (Pegion et al., 2019).

The forcing of hydrological models with subseasonal climate predictions to generate streamflow forecasts is a state-of art scientific field with recent publications worldwide (McInerney et al., 2020; Cao et al., 2021; McInerney et al., 2022; Tiwari& Mishra; 2022). However, it has also been little explored in Brazil with only one scientific paper about streamflow prediction using subseasonal GCMs (Quedi & Fan, 2020.).

The main objective of this work is to propose a mutimodel ensemble approach to generate monthly probabilistic streamflow forecasts from a hydrological model forced by both NMME and SUBX predictions for all the 87 hydropower catchments that are monitored by the electrical system's operator in Brazil. This work also seeks to present an extensive review of the literature of dynamic seasonal streamflow forecasting in Brazil to reveal the existing literature gap.

## **2. REVIEW OF DYNAMIC STREAMFLOW FORECASTING IN BRAZIL**

We carried out a literature overview about seasonal streamflow forecasting in Brazil to identify the existing gap in dynamic streamflow forecasting. The review was performed by manual text mining using the Google Scholar database, focusing on the period from 2014 to 2023. The search query included the terms: Brazil seasonal "streamflow forecast". We limited the search to articles written in English and Portuguese languages. Table 1 presents the summary of the literature review.

To classify the results of the literature review, the retrieved articles were categorized into three groups: Statistical, Dynamical, and Irrelevant. The classification was based on the nature of the research, focusing on whether it pertained to statistical streamflow forecasting, dynamical streamflow forecasting, or irrelevant if the retrieved article was not about streamflow forecasting.

The classification process involved reviewing each article and determining its relevance according to its object of study being a Brazilian catchment, its thematic alignment, and the



temporal scale of the research (specifically monthly scale). Table 1 provides a year-by-year breakdown of the classification results for all the articles found in the literature review. It presents the publication year of each article, along with its assigned classification (Statistical, Dynamical, or Irrelevant).

Table 1 – Classification of the retrieved articles

Year	Query Results	Statistical	Dynamical	Irrelevant
2023	35	4	2	29
2022	76	1	0	75
2021	74	3	0	71
2020	56	5	1	50
2019	52	3	0	49
2018	39	2	0	37
2017	35	1	0	34
2016	30	2	1	27
2015	28	0	1	27
2014	23	0	0	23
<b>Total</b>	<b>448</b>	21	5	422

The classification process identified five articles that were classified as Dynamical. These articles are summarized in Table 2. Except for Greuell and Hutjes (2023), all Dynamical articles are from the same research Group in Brazil – Instituto de Pesquisas Hidraulicas (IPH-RS).

None of these articles have used the NMME as the climate ensemble and none were conducted at a national scale, indicating a more localized (for the cases of catchment and regional scale) or generalized (for the case of continental scale) focus in their study areas.

Additionally, none of these articles employed any specific strategy to compose a multimodel ensemble for streamflow forecasting purposes.

Table 2 – Summary of the articles about dynamical monthly streamflow prediction in Brazil

Authors	Climate Model	Hydrological Model	Spatial Scale
Fan et al. (2015)	TIGGE	MGB-IPH	Regional
Fan et al. (2016)	ECMWF	MGB-IPH	Catchment
Quedi and Fan (2020)	ECMWF - S2S	MGB-IPH	Regional
Ávila et al. (2023)	ECMWF	Multiple	Catchment
Greuell and Hutjes (2023)	ECMWF - SEAS5	VIC	Continental

### 3. CASE STUDY AND OBSERVED DATA

The observed streamflow dataset includes naturalized monthly streamflow series from the 87 monitored hydropower sites in Brazil, spanning the period from 1932 to 2020. These streamflow measurements have been obtained by ONS (Brazilian System Operator) and are the series used in the planning and management of the Brazilian electrical sector. The catchment areas of these sites range from 322 to 823,555 square kilometers. The spatial distribution of the hydropower sites is presented in Figure 1.

To obtain the naturalized streamflow series, ONS applies a consolidation and consistency process. This process involves the removal of reservoir operations upstream of the streamflow gauges, as well as the estimation and addition of evaporation from hydropower

reservoirs and water withdrawals across the reservoir basin.

The precipitation dataset is a  $0.25^\circ \times 0.25^\circ$  grid obtained from the interpolation of the rainfall gauges available from the National Water Agency public database. The precipitation time series are for the 1960 to 2020 period. The evapotranspiration dataset is a  $0.25^\circ \times 0.25^\circ$  grid obtained from the interpolation of the meteorological gauges available from the Instituto Nacional de Meteorologia (Inmet) public database. In this study, the hydrological modeling procedure solely utilized the historical monthly mean of the evapotranspiration time series. Other variations or temporal aspects of evapotranspiration were not considered for the analysis.

Figure 1 – Brazilian Monitored Hydropower Sites.



#### 4. METHODOLOGY

The proposed multimodel approach for monthly streamflow forecasting in the Brazilian electrical sector basins is detailed in Figure 2. It can be described as an eight-step procedure:

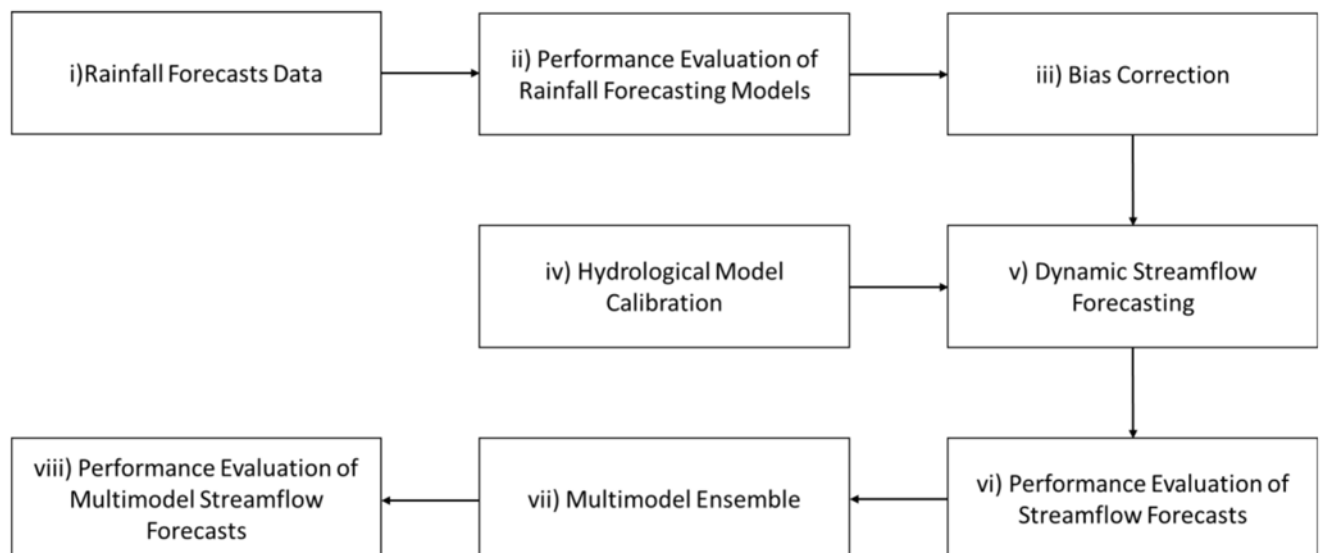
- i. Acquisition of Rainfall Forecasts Data. The process of acquiring rainfall hindcasts from both the NMME and SubX models is undertaken. The NMME models provides monthly rainfall hindcast with 1 to 12 months lead times while the SUBX offer daily-scale rainfall hindcasts with lead times ranging from 1 to 42 days.

- ii. **Performance Evaluation of Rainfall Forecasting Models.** To assess the performance of the rainfall forecasting models, a correlation analysis is conducted between the raw rainfall forecasts and the observed data. This analysis is carried out on the models' original grid.
- iii. **Bias Correction.** A bias correction technique called quantile mapping is employed. This approach helps to mitigate any systematic biases present in the forecasts.
- iv. **Hydrological Model Calibration.** The hydrological model parameters for each catchment are determined through an optimization procedure. This calibration process involves adjusting the model parameters to improve their agreement with observed data and ensure the accuracy of the hydrological model's predictions for each specific catchment.
- v. **Dynamic Streamflow Forecasting.** The optimized hydrological models for each catchment are utilized to generate monthly streamflow forecasts. These models are driven by the previously acquired and processed rainfall forecasts. By incorporating the rainfall forecasts as inputs, the hydrological models simulate the expected streamflow patterns for the upcoming months.
- vi. **Performance Evaluation of Streamflow Forecasts.** The performance of the streamflow forecasts is evaluated using established metrics to assess their accuracy and reliability. These metrics are applied to compare the performance of different forecasting models for each catchment. In addition, the streamflow forecasts are benchmarked against a naïve model, which serves as a reference baseline. This comparison allows for the assessment of the extent to which the streamflow prediction performance of each model improves or outperforms the simplistic naïve model. By conducting these evaluations, it becomes possible to

identify the models that offer significant performance gains in streamflow prediction for each specific catchment.

- vii. **MultiModel Ensemble.** The multimodel ensemble is constructed by assigning weights to each model based on their individual performance. These weights are determined proportionally, considering the relative performance of each model in generating accurate streamflow forecasts. The higher the performance of a model, the greater its weight in the ensemble. This weighting process ensures that the probability forecasts incorporate the strengths of each individual model, providing a more robust forecast.
- viii. **Multimodel Performance.** The multimodel streamflow forecasts performance is determined to verify if there is gain in using the multimodel against the best model for each basin and against the baseline. The performance is based on a cross validation procedure.

Figure 2 – Flowchart of the multimodel monthly streamflow forecasting procedure.



#### 4.1. Acquisition of Rainfall Forecasts Data

The North American Multi-Model Ensemble (NMME) is a collaborative project involving several modeling centers in North America that contribute with forecasts of various

climate variables, such as precipitation and temperature. The forecasts are publicly available on a global scale in the NMME project webpage, represented on a grid with a resolution of 1° latitude by 1° longitude. The lead times of these forecasts range from 0.5 to 11.5 months, providing valuable information for medium to long-term climate predictions.

The participating modeling centers contribute both hindcasts, which are retrospective forecasts, dating back to the early 1980s, as well as real-time forecasts. The hindcasts and forecasts are stored in an online repository from the International Research Institute for Climate and Society (IRI) (<http://iridl.ldeo.columbia.edu/SOURCES/.Models/.NMME/>), from which the monthly rainfall hindcasts were obtained for all the six active models. The characteristics of the currently active NMME models are summarized in Table 3.

Table 3 – Summary of the active NMME models.

Model	Institution	Hindcast Period	Lead time (months)	Members
CanCM4i-IC3	CMC	[Jan 1980,Nov 2021]	0.5-11.5	10
GEM5-NEMO	CMC	[Jan 1980,Nov 2021]	0.5-11.5	10
GFDL-SPEAR	GFDL	[Jan 1991,Nov 2021]	0.5-11.5	30
NASA-GEOSS2S	NASA	[Feb 1981,Sep 2017]	0.5-9.5	4
COLA-RSMAS-CCSM4	NCAR	[Jan 1991,Nov 2021]	0.5-11.5	10
NCEP-CFSv2	NCEP	[Jan 1982,Sep 2011]	0.5-9.5	24

The Subseasonal to Seasonal Prediction Project (SUBX) is another collaborative initiative involving multiple modeling centers in North America. It provides publicly available subseasonal daily forecasts on a grid with a resolution of 1° latitude by 1° longitude with lead time up to 45 days. Its hindcasts and forecasts are also stored in an online repository from IRI (<http://iridl.ldeo.columbia.edu/SOURCES/.Models/.SubX/>). We used daily rainfall hindcasts from three SUBX models. The chosen SUBX models are summarized in Table 4. As this study

focus in the monthly scale, the SUBX daily rainfall hindcasts were aggregated into monthly forecasts. For a particular month, its forecasts were aggregated by considering the forecasts that were produced in the last week of the previous month.

Table 4 – Summary of the chosen SUBX models.

Model	Institution	Hindcast Period	Lead time (days)	Members
ESRL-FIM	ESRL	[Jan 1999,Nov 2021]	0.5-34.5	4
EMC-GEFS	EMC	[Jan 1999,Nov 2021]	0.5-34.5	11
NCEP-CFSv2	NCEP	[Jan 1999,Nov 2021]	0.5-44.5	4

#### 4.2. Performance Evaluation of Rainfall Forecasting Models

The primary measure used for evaluation is the anomaly correlation (AC), which quantifies the association between the anomalies of forecasted values at gridpoints and corresponding observed values. The observed values were regridded to match the  $1^\circ \times 1^\circ$  models' grid, all the models were available on the same  $1^\circ$  latitude by  $1^\circ$  longitude grid by the online repository from IRI. No distance performance measure like root-mean-square error (RMSE) is considered in this step as raw climate forecasts are biased.

The monthly rainfall forecast skill is assessed for all NMME and SUBX models by calculating the AC for each model's ensemble mean (EM). The performance evaluation period is from January 1991 to December 2016 as it is the longest common period for all models. The analysis is focused on the 0.5 lead (LAG 1), as it is the common lead between the NMME and SUBX models.

Beside the performance of each individual model and its spatial distribution in Brazil, this step aims to determine whether the inclusion of subseasonal models provides enhanced



monthly rainfall forecasting capabilities compared to using only the NMME models. This information aids in determining which models should be prioritized and included in the streamflow forecasting procedures, as models with higher performance are likely to contribute more accurate and reliable streamflow predictions.

### 4.3. Bias Correction

The initial process in this step involves transforming the raw rainfall forecasts from the  $1^\circ \times 1^\circ$  grid resolution to the catchment scale. This procedure is accomplished for each catchment using the Thiessen polygons. The interpolation by Thiessen polygons considers the spatial proximity of the models' data points to the catchment, assigning higher weights to nearby locations and lower weights to more distant ones.

Then, the raw climate data at catchment scale is bias corrected by the Quantile Mapping (QM) technique. QM is a statistical technique used to align the cumulative distribution functions (CDF) of two data series. This method derives the mapping function by comparing the quantiles of the two data series. For bias correction, QM in its general form can be written as:

$$P_c = F_o^{-1}(F_m(P_m)) \quad (1)$$

where  $P_c$  is the bias corrected variable,  $F_o^{-1}$  is the inverse of the CDF corresponding to the observations,  $F_m$  is the CDF of the GCM forecasts,  $P_m$  is the GCM forecast.

In this study, the Quantile Mapping (QM) procedure was implemented assuming that the cumulative distribution function (CDF) of both the observed data and the models' forecasts follows a Gamma distribution. The Gamma distribution is a two-parameter continuous probability distribution that is often used to model monthly rainfall as it is a non-negative and positively skewed.

Due to the existence of seasonality in monthly rainfall data, the QM procedure is applied

to each month separately. The parameters of the Gamma CDFs were adjusted by the maximum likelihood method for each month for both the observation and forecasts data. This step results in the bias corrected monthly rainfall forecasts for each catchment.

#### **4.4. Hydrological Model Calibration**

In this work, we used the hydrological model Soil Moisture Accounting Procedure (SMAP) which is a well-accepted model by the Brazilian hydrology community. It has been applied to various basins within Brazil (Block et al., 2009; Kwon et al., 2012; Cavalcante et al., 2020).

SMAP, which was developed by Lopes et al. (1982), is a conceptual and lumped hydrological model that represents soil processes into two reservoirs (subsurface and groundwater). It relies on four key parameters: soil saturation capacity, surface flow, a recharge coefficient, and a base flow recession coefficient. SMAP requires catchment area and monthly basin-average precipitation and evapotranspiration as input data.

The hydrological modeling procedure solely utilized the historical monthly mean of the evapotranspiration time series from Inmet stations. Other variations or temporal aspects of evapotranspiration were not considered for the analysis.

We calibrated the parameters of the SMAP model for each catchment using the DREAM algorithm (Vrugt et al., 2008). DREAM (DiffeRential Evolution Adaptive Metropolis) is a Bayesian inference algorithm commonly used for parameter estimation in hydrological modeling. By employing a Bayesian approach, uncertainties associated with model parameters can be quantified and accounted for in subsequent analyses. A 18 month warming up period was considered in the calibration and simulation of the model.

The objective function of the calibration procedure is the minimization of the difference between the model response and observation. We calibrated the model for the period Jan-1981 to Dec-2010, and the validation period was Jan-2011 to Dec-2016. The validation procedure

was based on the Nash Sutcliffe Efficiency (NSE) defined as follows:

$$NSE = 1 - \sum \frac{(Q_o - Q_m)^2}{(Q_o - \bar{Q})^2} \quad (2)$$

where,  $Q_o$  is the observed streamflow,  $Q_m$  is the modeled streamflow,  $\bar{Q}$  is the mean of the observed streamflow.

NSE quantifies the agreement between observed and model-generated values, with a range of values from 1 to negative infinity ( $-\infty$ ). In an ideal scenario where the model response perfectly matches the observations, the NSE attains a value of unity (1). Conversely, negative NSE values indicate that the mean observed value ( $\bar{Q}$ ) provides a better estimate than the model response.

According to Moriasi et al. (2007), NSE values around 0.5 or greater are generally considered satisfactory for hydrological modeling. These values imply a reasonable level of agreement between the model outputs and the observed data.

#### **4.5. Dynamic Streamflow Forecasting**

The monthly streamflow forecasts are generated by forcing the warmed up and optimized hydrological models with the bias corrected monthly rainfall forecasts for each catchment. This results in the forecasted streamflow series for each catchment, model and ensemble member.

#### **4.6. Performance Evaluation of Streamflow Forecasts**

We evaluated the performance of the ensemble streamflow forecasts by each model for each catchment using a discrete probabilistic method used by IRI (IRI, 2013): the Rate of Return (RR) performance index, the metric considers the climatology as a naïve model for defining if there are prediction skill gains. For the application of the discrete metrics, the streamflow forecasts were classified into three classes: i) Normal, percentiles ranging from 33% to 66%; ii) Above Normal, percentiles ranging from 66% to 100%; iii) Below Normal, percentiles ranging from 0% to 33%. The percentiles are defined based on the empirical distribution of the mean of

each ensemble model and are defined for each month.

The RR score is a metric that evaluates the performance of forecasts based on their ability to assign high probabilities to observed outcomes. This score is defined as:

$$RR = \frac{L_{for}}{L_{clim}} - 1 \quad (3)$$

where RR is the Rate of Return score of the forecasts and  $L_{clim}$  is the Likelihood score of the climatology. The likelihood score (L) is determined as:

$$L = \prod_{i=1}^n \sqrt[n]{p_i} \quad (4)$$

where  $p_i$  is the probability assigned by the model to the observed class in the prediction date  $i$  and  $n$  is the number of prediction dates.

The Rate of Return measures the agreement between the forecasted probabilities and the observed outcomes. It quantifies the forecast's ability to assign higher probabilities to the observed outcomes, indicating its discriminatory power. The climatology score represents the probabilities based solely on historical climatic averages, without considering the forecast information.

The RR is defined such that a value of 0 indicates no-skill forecasts, while positive values indicate gains in forecasting skill against the naïve model, the climatology. Negative values are obtained when the likelihood score for the forecasts is lower than the score of the climatology.

#### 4.7. Multimodel Ensemble

The multimodel ensemble aims to create a posterior probability forecast by combining predictions from various models along with a climatological forecast, the climatological forecast is a naïve forecast model in which all of its predictions are equal to the monthly average value of the historical series. The combination of these predictions is determined by assigning weights to each model and to the climatological forecast. We used the multimodel formulation

from Robertson et al. (2004). The expected value of each class of a Multimodel Ensemble with  $J$  different models plus a climatological forecast can be mathematically expressed as:

$$E (MM_{kt}) = \frac{\sum_{j=1}^{J+1} w_j m_j p_{jkt}}{\sum_{j=1}^{J+1} w_j m_j} \quad (5)$$

where  $E(MM_{kt})$  is the expected value of the multimodel ensemble for the class  $k$  at time  $t$ ,  $w_j$  is the weight of the model  $j$ ,  $m_j$  is the size of the ensemble (equals to the number of years for climatology),  $p_{jkt}$  is the probability of the class  $k$  at time  $t$  for the model  $j$ .

The weights are constrained to positive values and are normalized to have sum equal to 1 by:

$$w_j = \frac{w_j}{\sum_{j=1}^{J+1} w_j} \quad (6)$$

The optimal weights are determined by the maximization of the likelihood. Similar to the likelihood score, the likelihood of the multimodel can be written as:

$$L = \prod_{t=1}^N \sqrt[N]{E(MM_{k^*t})} \quad (7)$$

Where,  $N$  is the length of the calibration period and  $k^*$  is the category actually observed at time  $t$ .

The optimization of the parameters is conducted for each catchment during the common period of all models, which spans from January 1999 to December 2010. The optimization procedure was carried out using the Particle Swarm Optimization (PSO) method.

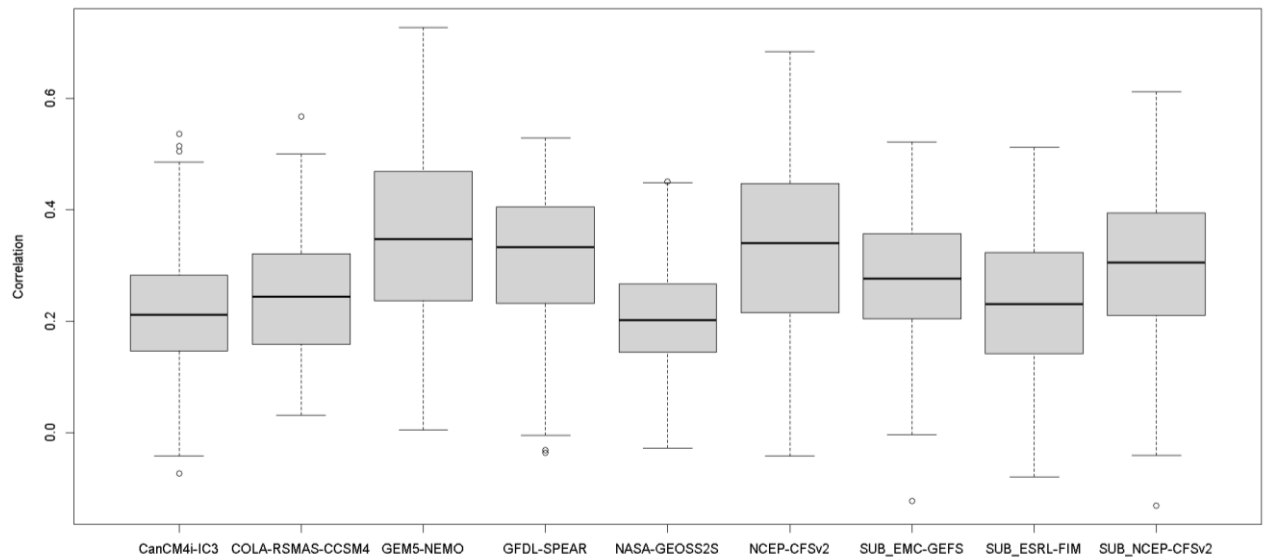
To evaluate the performance of the Multimodel, a cross-validation procedure was applied where each year was sequentially removed during the weight calibration process. The forecasts of the multimodel for each year that was not part of the calibration of its weights was considered for the validation set.

## 5. RESULTS

### 5.1. Performance Evaluation of Rainfall Forecasting Models

The performance assessment of the raw rainfall forecasting models is depicted in Figure 3, which showcases the correlation coefficient between the observed and modeled data in the models' grid. The boxplot representation provides insights into the dispersion across multiple grid cells. Overall, the models exhibited moderate correlation, with median values ranging from [0.2-0.35], and maximum correlation values ranging from [0.5-0.75]. Both the NMME and SUBX models demonstrated comparable performance, suggesting that the integration of SUBX models within the multimodel framework could potentially enhance the overall forecasting performance.

Figure 3 – Pearson Correlation Coefficient of the Precipitation forecasting models and the observed data for 1 month lead time.



The performance spatial distribution is illustrated in Figure 4 which depicts the correlation coefficient of the best model (i.e. the model with greatest correlation coefficient) for each grid cell. The Northeast region presented the overall highest performance with the presence of strong correlation coefficients ( $>0.6$ ), The South region and the northern part of the Southeast region presented medium to high correlation coefficients. The lowest correlations are

found in the western parts of Brazil.

The spatial distribution of the optimal model is depicted in Figure 5. Among the considered models, the Canc4i-IC3 NMME model did not emerge as the top-performing model for any grid cell, while the NASA-GEOSS2S NMME model achieved the highest performance for only one grid cell. In contrast, the GEM5-NEMO NMME model exhibited the most frequent occurrence, being identified as the best model for approximately 35% of the grid cells. The SUBX models demonstrated notable performance, with approximately 25% of the grid cells recognizing them as the best model. Among the SUBX models, the SUB\_NCEP-CFSv2 appeared most frequently as the top-performing model, encompassing around 15% of the grid cells.

Figure 4 – Pearson Correlation Coefficient of the best precipitation forecasting model in each grid cell for 1 month lead time.

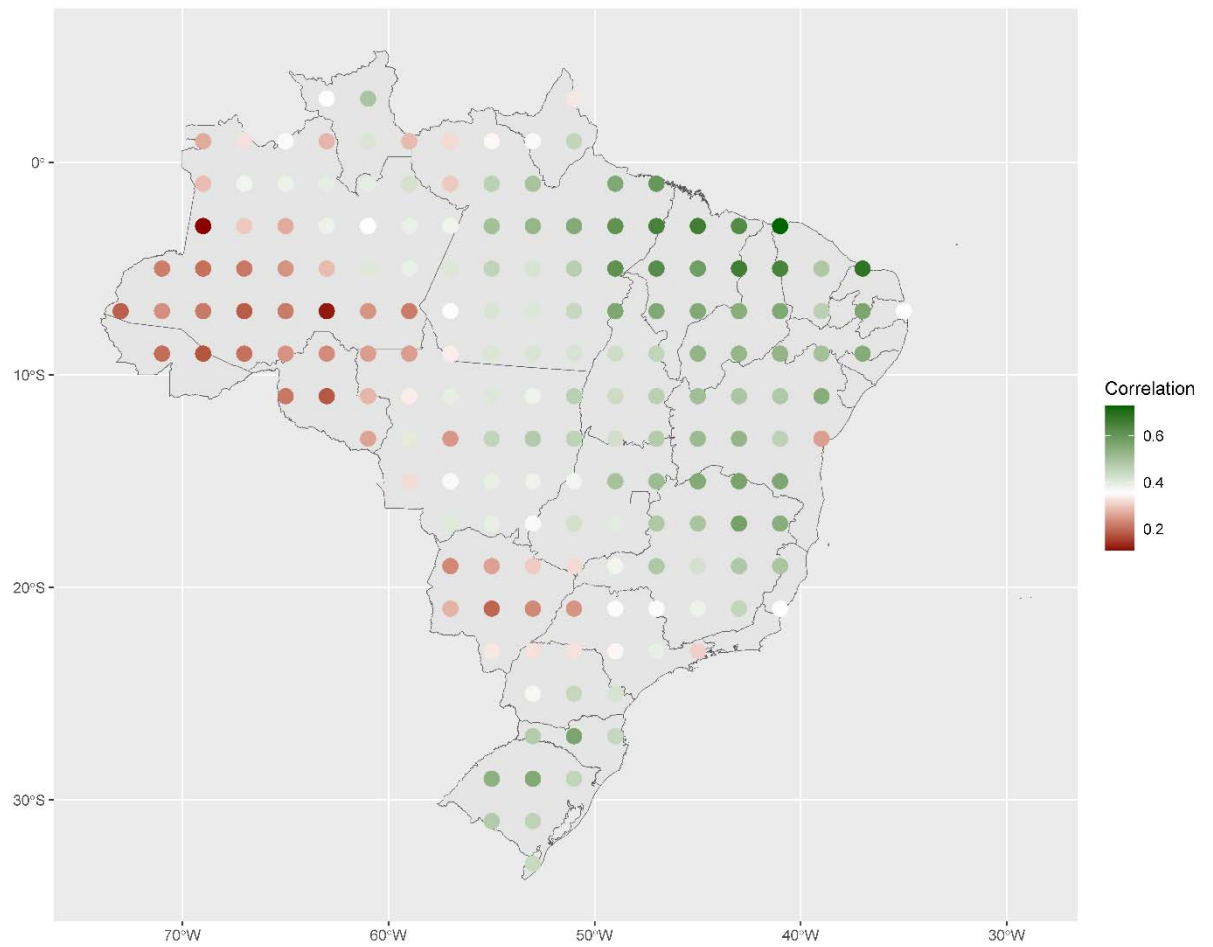
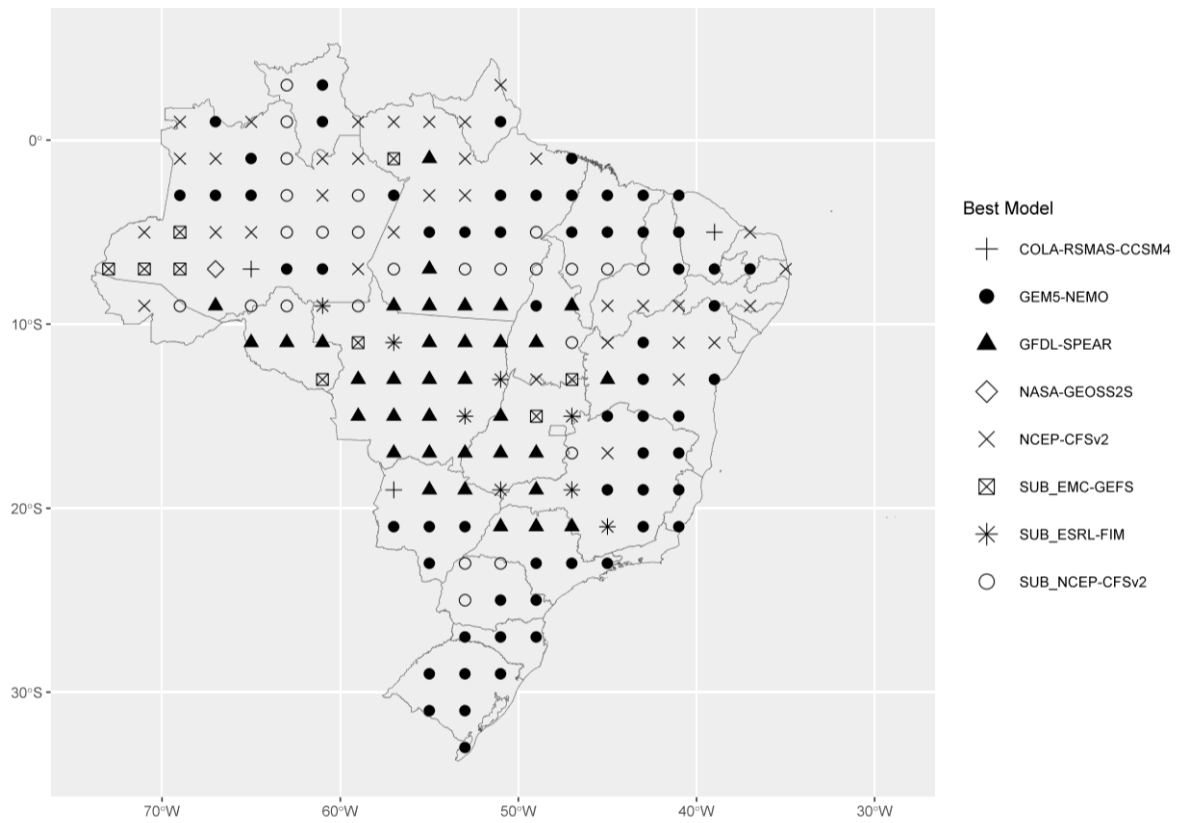


Figure 5 – Highest correlation model of the best precipitation forecasting model in each grid cell for 1 month lead time.





## 5.2. Performance Evaluation of the Hydrological Modeling

The performance of hydrological modeling is depicted in Figure 6, showcasing the boxplot of Nash-Sutcliffe Efficiency (NSE) values for both the calibration and validation periods across different catchments. Figure 7 illustrates the spatial distribution of NSE values for hydrological modeling. During the calibration period, the modeling procedure demonstrated excellent overall performance, with a median NSE of 0.75 and low dispersion. In the validation period, the median NSE decreased to 0.69 with higher dispersion. Despite the overall strong performance, approximately 14% of the catchments exhibited negative NSE values during the validation period.

Figure 6 – Boxplot of the Hydrological Modeling NSE for both calibration and validation periods.

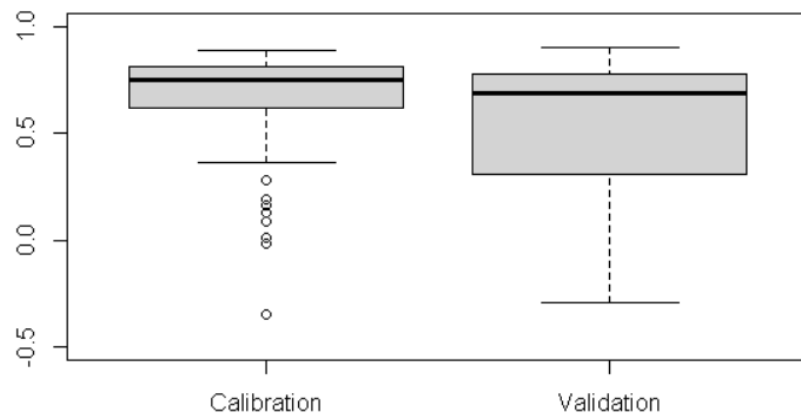
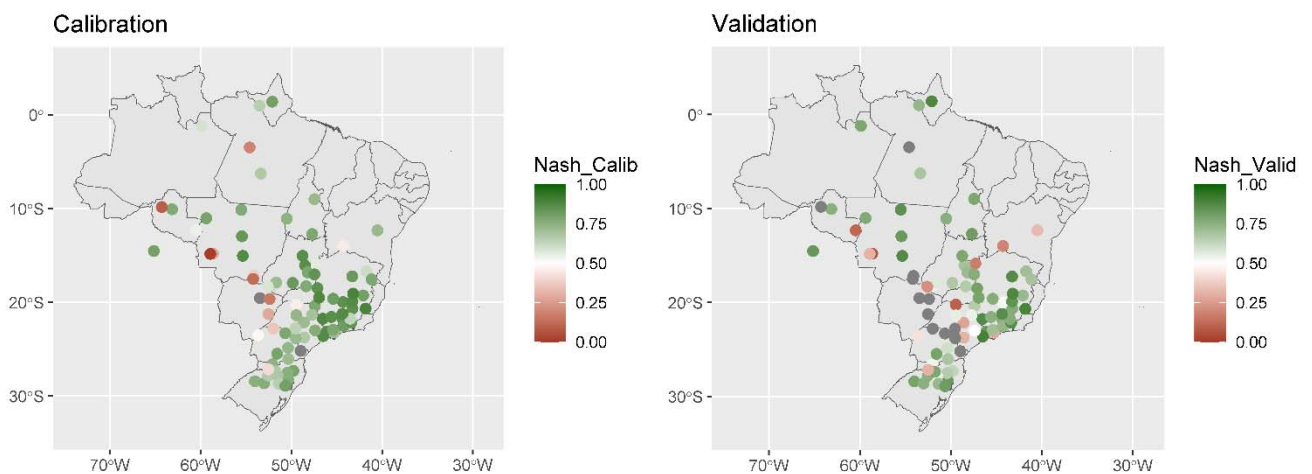


Figure 7 – Spatial Distribution of Hydrological Modeling NSE for Each Catchment for both Calibration and Validation periods.



### 5.3. Individual Models Performance Evaluation of the Monthly Streamflow Forecasts

The performance of the streamflow predictions from the individual NMME and SUBX models is illustrated in Figure 8. It presents the boxplot of the Rate of Return performance index for streamflow predictions across various catchments for each GCM. Additionally, it also presents a boxplot featuring the streamflow predictions of the best performing model in each catchment.

The presented models demonstrated varied performance, but overall, the performance was low, with negative Rate of Returns observed in most basins. Among the NMME models,

both GEM5-NEMO and NCEP-CFSv2 exhibited the best overall performance, while NASA-GEOSS2S displayed the worst. The SUBX ECM-GEFS model showcased performance similar to the NMME models. On the other hand, the ESRL-FIM and NCEP-CFSv2 SUBX models performed notably worse.

By utilizing the predictions from the best performing model in each basin, there is a substantial improvement in overall performance compared to considering individual models. Approximately 45% of the catchments show positive values of the Rate of Return index (i.e. better performance than climatology). In contrast, when considering the NCEP-CFSv2 NMME model, which was the best individual model, only 28% of the catchments exhibit positive Rate of Return values.

Figure 9 showcases the spatial distribution of the Rate of Return performance index for the best performing streamflow prediction model in each catchment. Observing the figure, it becomes evident that the streamflow predictions exhibited positive performance in the majority of Southeast basins and some Middle West basins. However, the South basins predominantly displayed neutral performance, while the North basins, both Northeast basins, certain Middle West basins, and the southern Southeast basins demonstrated negative performance.

Figure 10 illustrates the spatial distribution of the best performing model. It highlights the heterogeneity in the spatial distribution of the best model, with the NCEP-CFSv2 NMME model appearing most frequently as the best model. Additionally, it is noteworthy that although ECM-GEFS is the only SUBX model that achieved the best performance, it appeared with high frequency across all Brazilian regions.

Figure 8 – Boxplot of the Rate of Return of the streamflow predictions of the NMME and SUBX models across each basin. Best Model represents the boxplot of the streamflow prediction of the model that best performed in each catchment.

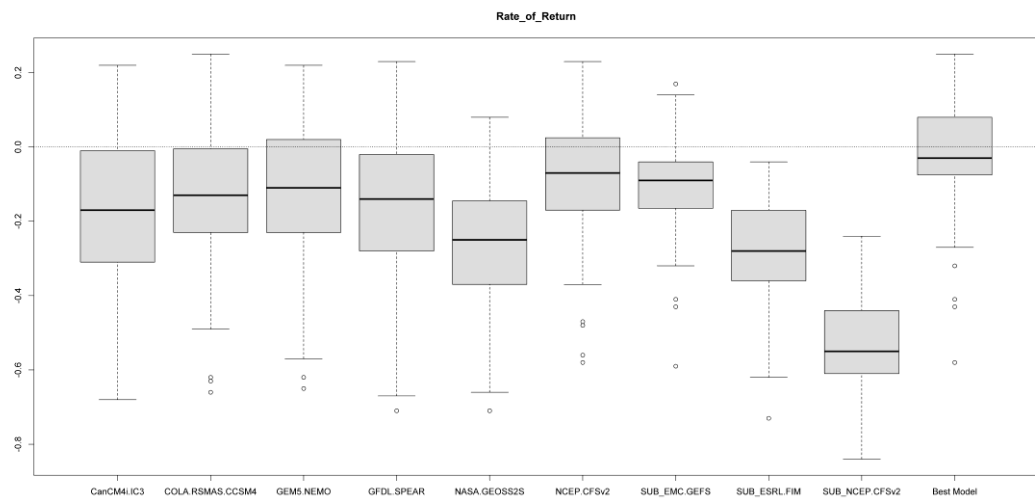


Figure 9 – Spatial Distribution of Rate of Return performance index for the best performing streamflow prediction model in each catchment.

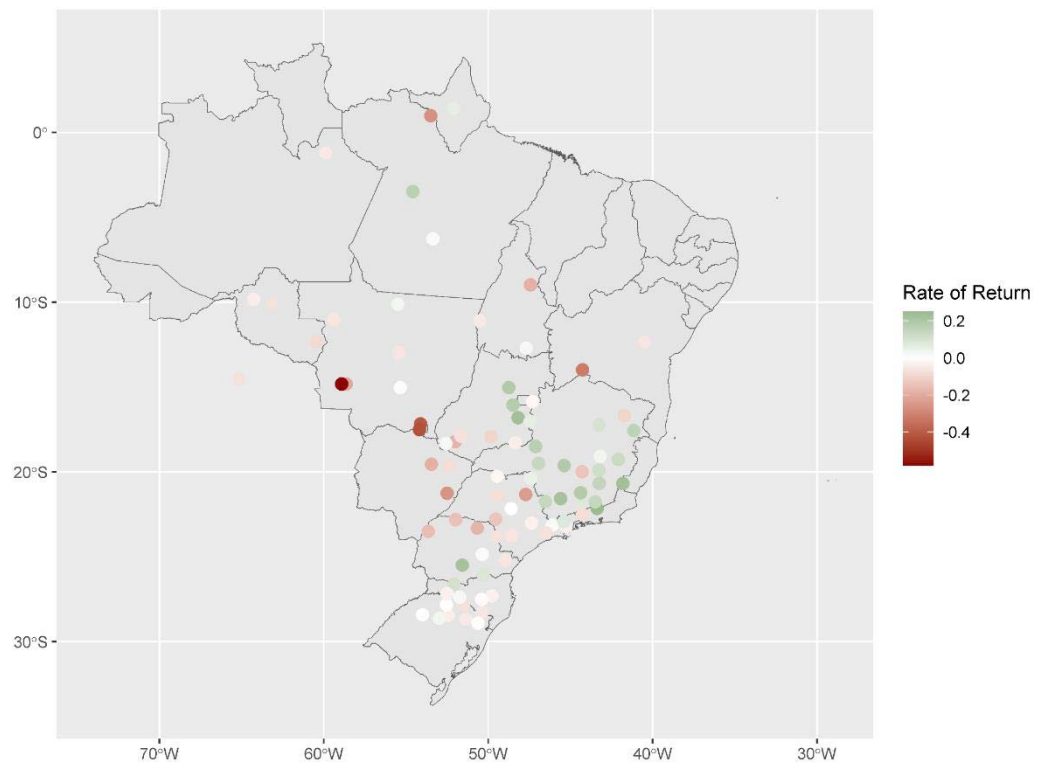
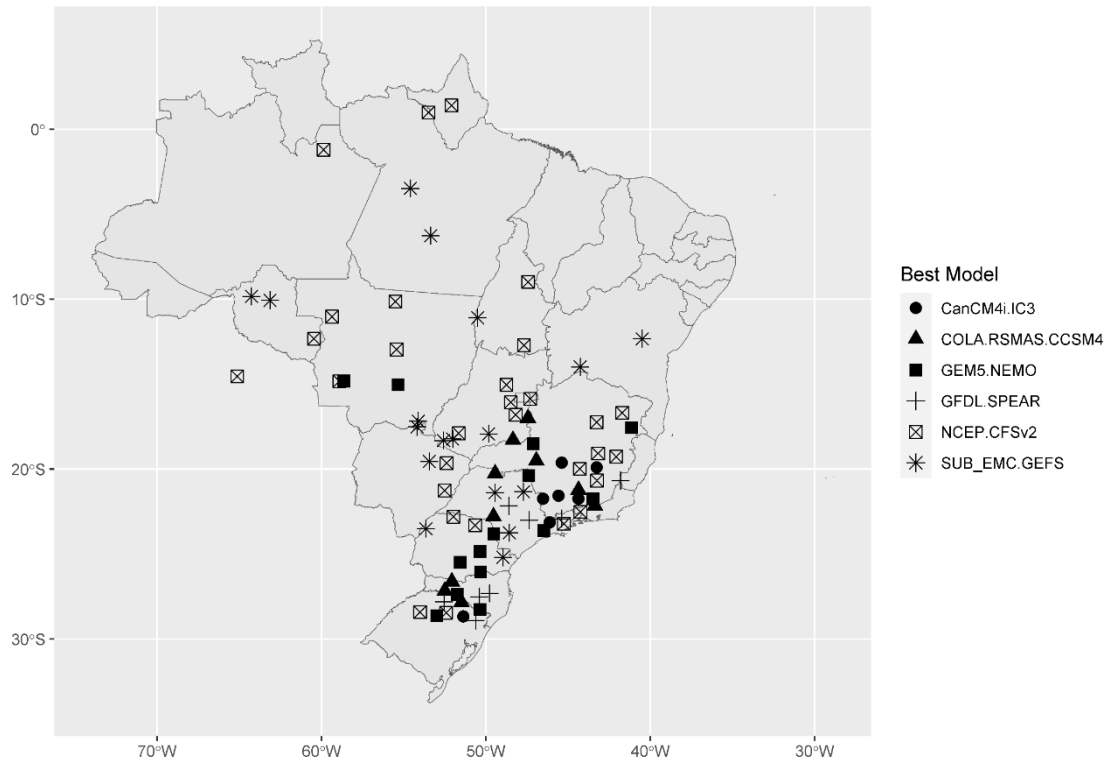


Figure 10 – Spatial Distribution of the best performing streamflow prediction model in each catchment.



#### 5.4. Performance Evaluation of the Multimodel Streamflow Forecats

The performance of the streamflow predictions from the individual models, from the best model composition and from the optimized Multimodel is illustrated in Figure 11. It presents the boxplot of the Rate of Return performance index for streamflow predictions across all the catchments.

The streamflow predictions obtained from the Multimodel approach exhibited superior performance compared to each individual model as well as to the composition of the best performing models. This increase in performance was significant across overall, maximum, and minimum values. It is worth highlighting that although the individual models did not demonstrate strong overall performance, their combination through the multimodel approach proved to be a robust forecasting model with significant positive Rate of Return values.

Figure 12 displays the weights of the models comprising the multimodel and their dispersion across the catchments. Several observations can be made:

- i) The climatology exhibits the highest overall weights among all the models.
- ii) The NMME models generally possess higher weights compared to the SUBX models in the overall composition.
- iii) Despite the NCEP-CFSv2 NMME model having the best individual performance and being the most frequently included in the best model composition, its overall weights in the Multimodel are lower compared to the other NMME models. Furthermore, its median weight is 0, indicating that its information was not considered in half of the catchments for the Multimodel composition.
- iv) Despite having the worst individual performance, the NCEP-CFSv2 SUBX model displays positive weights, with a median significantly different from 0. This suggests that it can

contribute additional information to the multimodel combination, even though its individual prediction did not exhibit notable forecasting skill.

Figure 13 presents the spatial distribution of the Rate of Return performance index for the Multimodel streamflow forecasts. In contrast to the individual models and the best model composition, the Multimodel predictions exhibit positive non-zero values for catchments across all Brazilian regions. However, the performance varies significantly with the location and the highest performance values are concentrated in the Southeast basins and the eastern Middle West basins. Moreover, unlike the individual models, the Northern region demonstrates some forecast skills in the Multimodel predictions.

Figure 14 displays the spatial distribution of the weights assigned to the Climatology "model" in the Multimodel forecasts. As anticipated, the weights of the Climatology model exhibit an inverse relationship with the performance of the Multimodel forecasts. When the Multimodel forecasts have zero performance values, it corresponds to the Climatology weights being close to 1. This indicates that the Multimodel considers that no other model, apart from the climatology, can contribute valuable information to the predictions.

Interestingly, in the South region, there are catchments with weights close to 0 for the climatology, despite not achieving strong performance in terms of the Rate of Return index. Conversely, in the Southeast region, there are catchments with high rate of return index values, indicating good performance, but with non-zero weights assigned to the climatology.

Figure 11 – Boxplot of the Rate of Return of the streamflow predictions of the NMME and SUBX models, the best performing model composition and the Multimodel predictions across each basin.

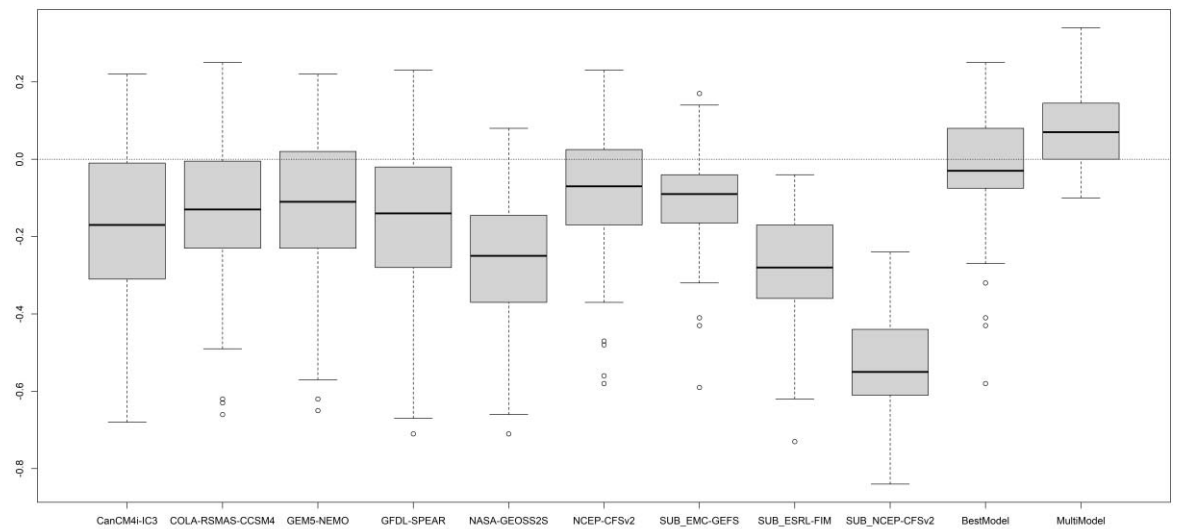


Figure 12 – Boxplot of the weights assigned to the models composing the multimodel across each basin.

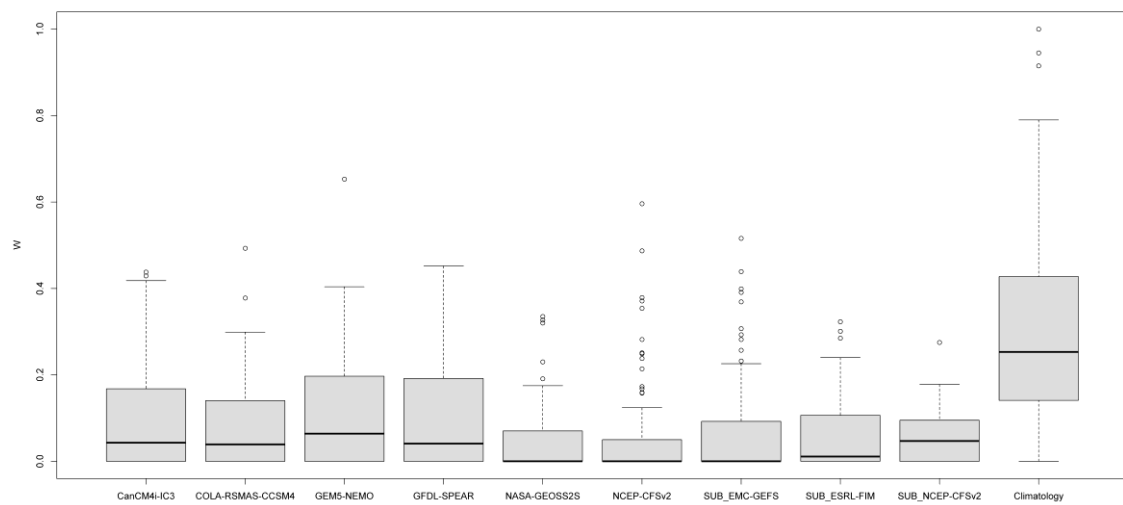


Figure 13 – Spatial Distribution of the Rate of Return performance index of the Multimodel Streamflow forecasts in each catchment.



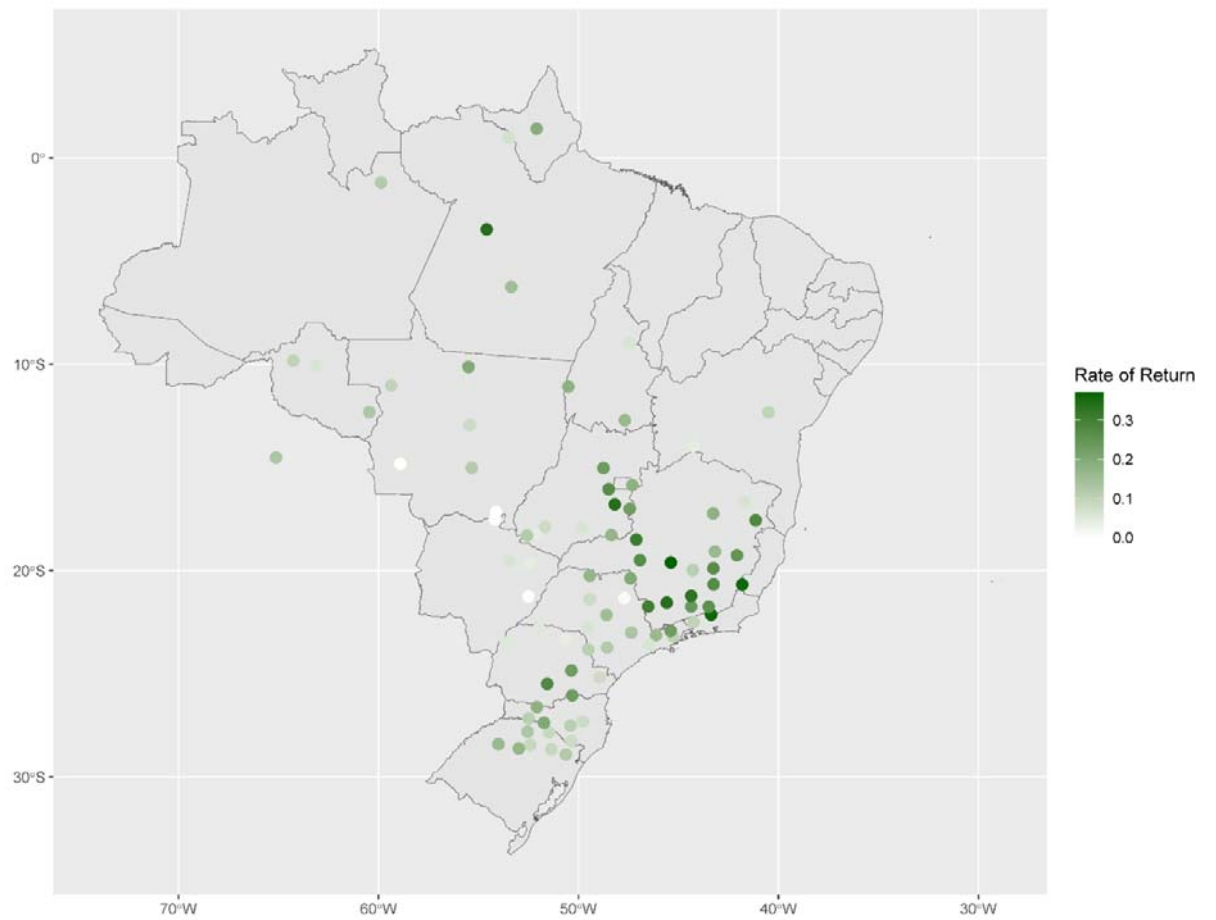


Figure 14 – Spatial Distribution of the weight assigned to climatology model in the Multimodel composition for each catchment.

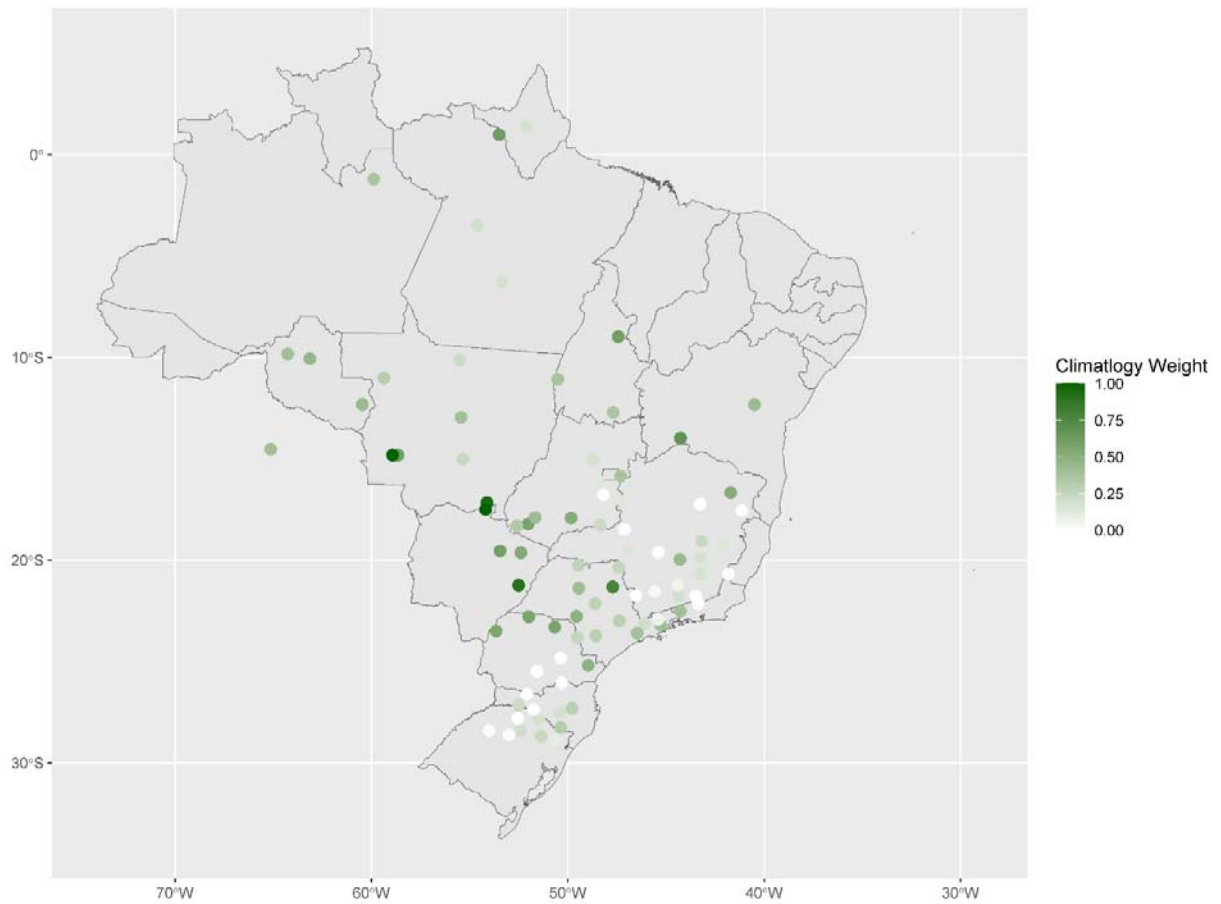


Figure 15 showcases the spatial distribution of the weights assigned to the NMME models by the Multimodel streamflow forecasts for each catchment. It can be noticed that: in contrast to other models, the CanCM4i-IC3 model exhibits non-zero weights for all regions except the Northeast region. Its highest weight values are primarily concentrated in the South, Southwest, and Middle West regions. It stands out as the model with the most non-zero weight values.

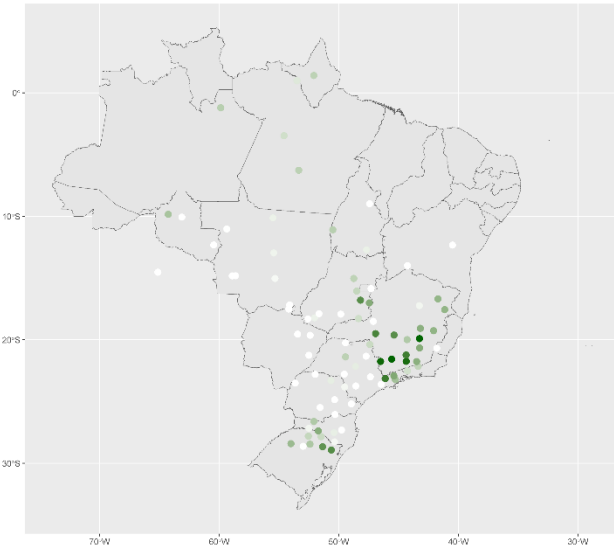
The NCEP-CSFv2 NMME model, on the other hand, has zero weights for most catchments. However, when it does have non-zero weights, they are notably high (e.g., 0.4). This emphasizes the model's significance for forecasts in the Middle-West region, particularly for the Tocantins-Araguaia River basin. For the Northeast region, all NMME models have zero weight values, except for the GEM5-NEMO model, which exhibits a low weight value of 0.18

for the Sobradinho catchment. This implies that the Multimodel streamflow forecasts do not rely on the NMME models for the catchments in the Northeast region.

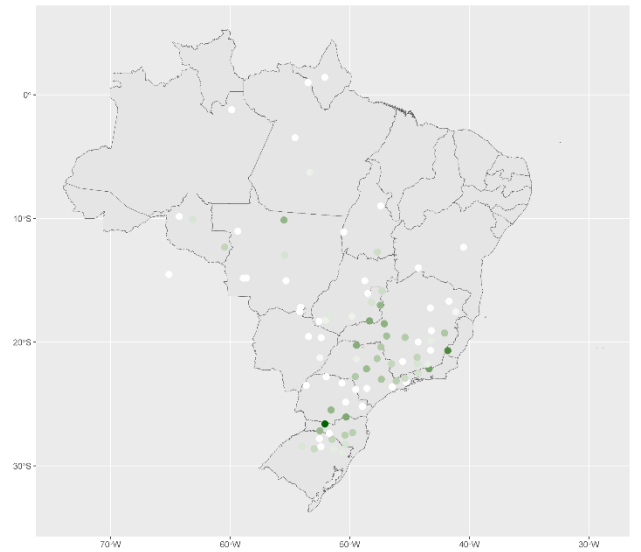
Figure 16 displays the spatial distribution of the weights assigned to the SUBX models by the Multimodel streamflow forecasts for each catchment. In general, the SUBX models exhibit weights close to 0 for most catchments. This suggests that the Multimodel streamflow forecasts rely less on the SUBX models compared to other models. Unlike the other SUBX models, the EMC-GEFS model does not have significant weight values for the South and Southeast regions. However, it does possess medium to high weight values for the Northeast and Midwest regions, it is the forecast model with highest weights for the Northeast Region. In contrast, the ESRL-FIM and NCEP-CFSv2 SUBX models exhibit higher weights for the South and Southeast regions.

Figure 15 – Spatial Distribution of the weights assigned to the NMME models by the Multimodel streamflow forecasts for each catchment.

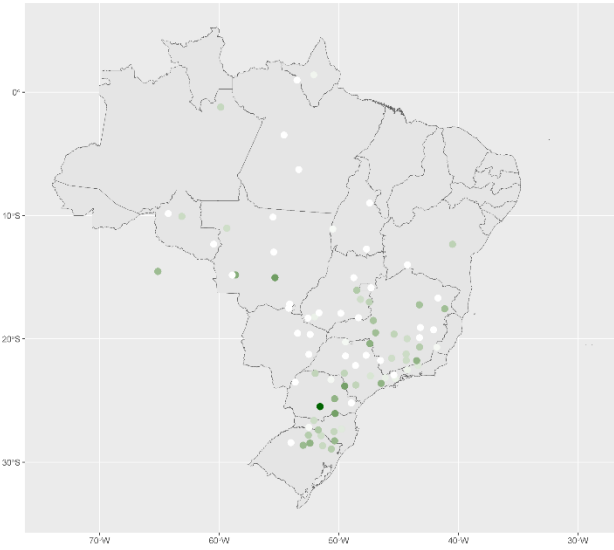
CanCM4+IC3



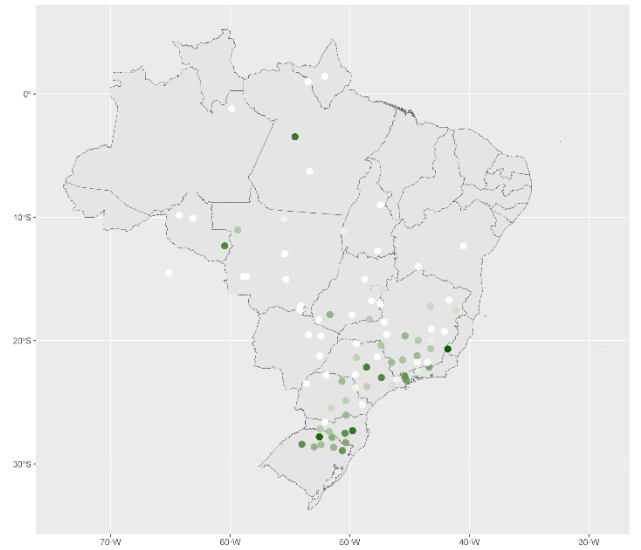
COLA-RSMAS-CCSM4



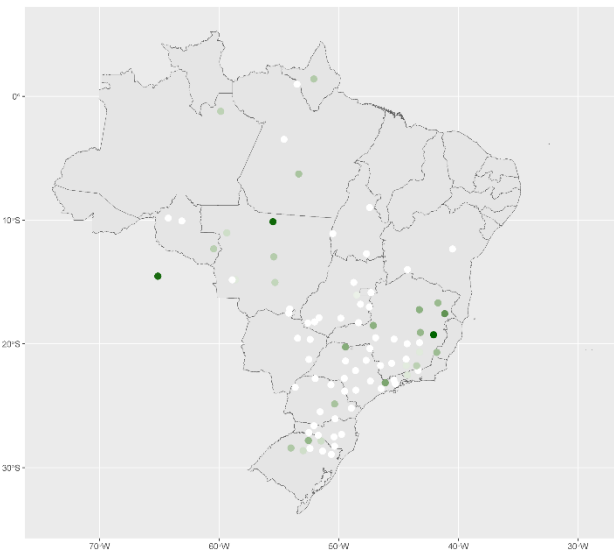
GEMS-NEMO



GFDL-SPEAR



NASA-GEOS2S



NCEP-CFSv2

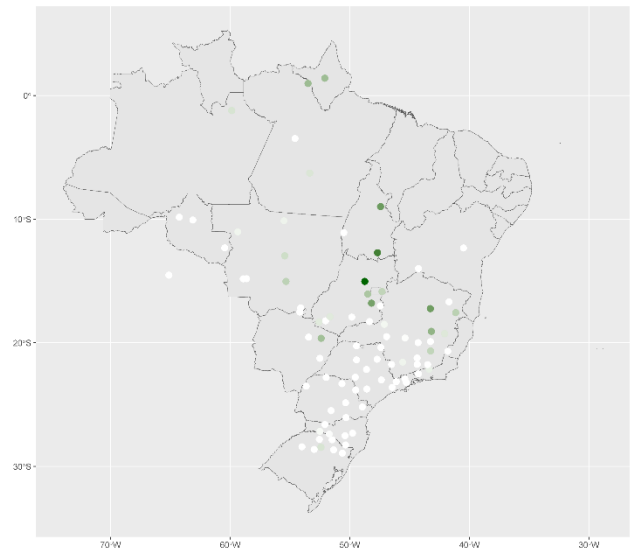
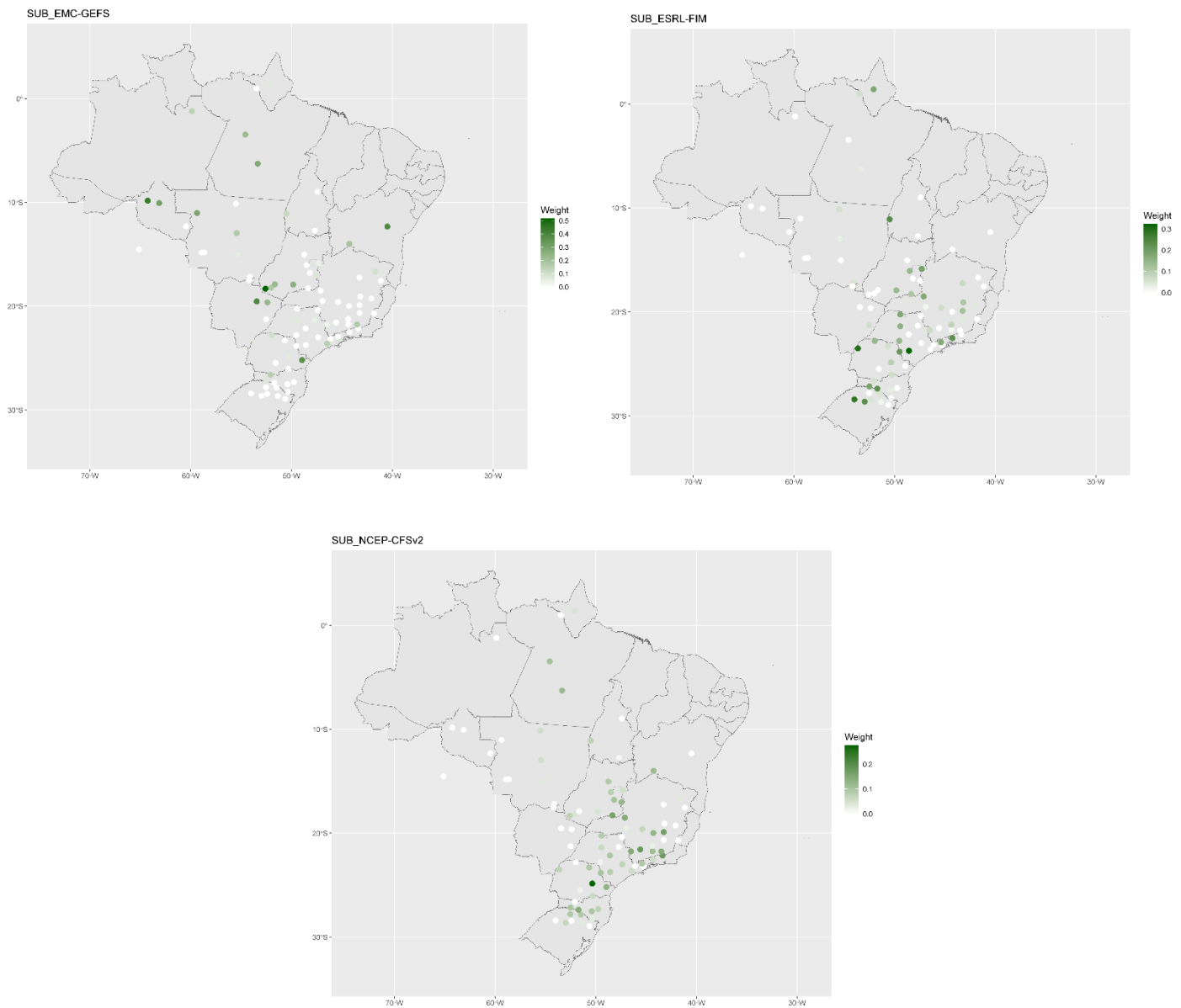


Figure 16 – Spatial Distribution of the weights assigned to the SUBX models by the Multimodel streamflow forecasts for each catchment.



## 6. DISCUSSION AND CONCLUSIONS

The findings of this study demonstrate that the combination of multiple forecast models into a Multimodel probability forecasting approach yields improved performance and greater

robustness compared to individual models, including the best individual model for each catchment. These results hold true for streamflow forecasting across all Brazilian regions. These findings align with previous studies such as Robertson et al. (2004), Tebaldi & Knuti (2007) for climate forecasting, and Najafi & Moradkhani (2016) for seasonal streamflow forecasting.

Furthermore, the study reveals that even individual models with poor performance can contribute to the overall performance of the Multimodel approach. It highlights that the best performing individual model is not necessarily the most crucial model for the multimodel compositions. These observations are consistent with the findings of Weigel et al. (2008) who demonstrated similar behavior using synthetically generated climate data.

The weights assigned to the SUBX models in the Multimodel streamflow forecasts suggest that, while they generally hold less importance compared to the NMME monthly forecast models, incorporating subseasonal models into a multimodel framework can enhance streamflow forecasts within a 1-month lead time, albeit with spatial dependence. Overall, this conclusion consistent with previous research conducted by Quedi & Fan (2020) and Zhou et al. (2023), reinforcing the notion that incorporating subseasonal models into a multimodel framework can enhance streamflow forecasts within a 1-month lead time, with the spatial dependence of their effectiveness.

The findings of this study provide strong evidence that the utilization of dynamical streamflow forecasting, although not commonly employed as statistical methods in Brazil, can significantly enhance the performance of monthly streamflow forecasting for the Brazilian hydroelectric sector. The results demonstrate positive performances for all regions and the majority of catchments. This highlights the value of dynamical streamflow forecasting in providing valuable insights and supporting better decision-making in the hydroelectric sector.

As future recommendations, we suggest incorporating climate models from other institutions, such as the ECHAM ensemble from the European Centre for Medium-Range

Weather Forecasts, into the multimodel framework. This recommendation stems from the study's findings, which demonstrated that the inclusion of different models can enhance prediction skills. By incorporating models from diverse sources, the multimodel framework can benefit from a wider range of perspectives and potentially improve overall forecast performance.

Additionally, we recommend developing a multimodel streamflow forecasting framework that integrates both statistical and dynamical models. This approach aims to leverage the strengths of both types of models to create a robust multimodel that can extract prediction gains from both statistical methods and climate forcing information.

## 4 CONCLUSION

The two studies presented in this doctoral thesis makes significant contributions to streamflow modeling and forecasting in Brazil, addressing both methodological and practical aspects. The first major contribution is in the methodological domain, where a novel statistical that couples GLM and copula technique for multisite streamflow simulation was proposed. This technique overcomes the limitations of traditional methods by incorporating various probability functions to model dependence structures, eliminating the need for normalization.

The method presented great performance for the Jaguaribe-Metropolitano basin in Ceará, Brazil, which presented unique challenges due to shallow soils and low short-term time dependency in streamflow series. The developed method can be used as an alternative to the classical methods with the flexibility being its greatest advantages. Although the methodology was initially developed for annual streamflow simulation, it can be easily extended to forecast monthly streamflow. Expanding the GLM-Copula to higher dimensions (beyond two spatially dependent time series) is also easily accomplished by integrating Generalized Linear Models (GLMs) for temporal dependence modeling with vine or maximum entropy copulas for spatial dependence modeling.

Despite the availability of numerous time series simulation methods, this research has identified opportunities for further advancements in this field. The investigation introduced a novel method that overcomes certain limitations of existing approaches. The proposed method exhibits qualities of intuitiveness, robustness, computational efficiency, and compatibility with widely accessible open-source R packages. Consequently, the authors posit that the proposed model holds potential for future studies and applications, owing to its flexibility and the performance is has demonstrated.

The second contribution of this thesis is specifically addressing the gap in monthly streamflow forecasting in Brazil. This contribution presented in the second article also introduces new advancements in streamflow forecasting for Brazil's hydropower sector by



using a hydrological model forced by both NMME and SUBX predictions for all the 87 hydropower catchments that are monitored by the electrical system's operator. One notable aspect is the application of a multimodel probabilistic approach, where weights of different models are optimized to compose a robust forecast. This strategy enhances the accuracy and reliability of monthly streamflow forecasts, catering to the specific needs of the Brazilian hydropower sector.

The thesis also evaluates the application of Sub-seasonal models for predicting monthly streamflow. The analysis of the weights assigned to the SUBX models in the Multimodel streamflow forecasts provides valuable insights into their contributions. It is evident that, in general, these models are assigned relatively less importance compared to the NMME monthly forecast models within the multimodel framework. However, the incorporation of subseasonal models into the multimodel framework yields improvements in streamflow forecasts within a 1-month lead time, although the effectiveness is spatially dependent.

We recommend developing a multimodel streamflow forecasting framework that integrates both statistical and dynamical state-of-art models, also we recommend the application of methods that can capture the long-term variability like the GLM-Copula for seasonal streamflow forecasting in national scale. We also recommend extending the presented methodologies for seasonal streamflow forecasts. This can be achieved by taking into account the forecast window of climate models, like the NMME, spanning from 1 to 12 months.

## REFERENCES

- Aas, K., Czado, C., Frigessi, A., Bakken, H., 2009. Pair-copula constructions of multiple dependence. *Insur. Math. Econ.* 44, 182–198.  
<https://doi.org/10.1016/j.insmatheco.2007.02.001>
- Alexandre, A.M., Martins, E.S., Clarke, R.T., Reis, D.S., 2005. Regionalização de parâmetros de modelos hidrológicos. *An. do XVI Simpósio Bras. Recur. Hídricos. ABRH. João Pessoa- PB, Brasil.*
- Alpettiyil Krishnankutty, B., Ganapathy, R., Sankaran, P.G., 2020. Non-parametric estimation of copula based mutual information. *Commun. Stat. - Theory Methods* 49, 1513–1527.  
<https://doi.org/10.1080/03610926.2018.1563180>
- Andreoli, R.V., Kayano, M.T., 2004. Multi-scale variability of the sea surface temperature in the Tropical Atlantic. *J. Geophys. Res. C Ocean.* 109, 1–12.  
<https://doi.org/10.1029/2003JC002220>
- Barros, F.V.F., Martins E.S.P.R., Souza Filho, F.A., 2013. Regionalização de parâmetros do modelo chuva-vazão SMAP das bacias hidrográficas do Ceará. In: Souza Filho FA et al (eds) *Gerenciamento de Recursos Hídricos no Semiárido*, 1st ed., Expressão Gráfica e Editora, Fortaleza, pp 186-207.
- Brechmann, E.C., Czado, C., 2015. COPAR - Multivariate time series modeling using the copula autoregressive model. *Appl. Stoch. Model. Bus. Ind.* 31, 495–514.  
<https://doi.org/10.1002/asmb.2043>
- Box, G. E. P., and Jenkins, G. M., 1976. *Time Series Analysis: Forecasting and Control*, revised ed. Holden-Day, San Francisco, California, USA.
- Chandler, R.E., 2005. On the use of generalized linear models for interpreting climate variability. *Environmetrics* 16, 699–715. <https://doi.org/10.1002/env.731>
- Chandler, R.E., Wheeler, H.S., 2002. Analysis of rainfall variability using generalized linear models: A case study from the west of Ireland. *Water Resour. Res.* 38, 10-1-10–11.  
<https://doi.org/10.1029/2001wr000906>
- Chen, L., Qiu, H., Zhang, J., Singh, V.P., Zhou, J., Huang, K., 2019. Copula-based method for stochastic daily streamflow simulation considering lag-2 autocorrelation. *J. Hydrol.* 578, 123938. <https://doi.org/10.1016/j.jhydrol.2019.123938>
- Chen, L., Singh, V.P., Guo, S., 2013. Measure of Correlation between River Flows Using the Copula-Entropy Method. *J. Hydrol. Eng.* 18, 1591–1606.  
[https://doi.org/10.1061/\(asce\)he.1943-5584.0000714](https://doi.org/10.1061/(asce)he.1943-5584.0000714)
- Chen, L., Singh, V.P., Guo, S., Zhou, J., Ye, L., 2014. Copula entropy coupled with artificial neural network for rainfall–runoff simulation. *Stoch. Environ. Res. Risk Assess.* 28, 1755–1767. <https://doi.org/10.1007/s00477-013-0838-3>

- Chen, L., Singh, V.P., Guo, S., Zhou, J., Zhang, J., 2015. Copula-based method for multisite monthly and daily streamflow simulation. *J. Hydrol.* 528, 369–384.  
<https://doi.org/10.1016/j.jhydrol.2015.05.018>
- Cover, T.M., Thomas, J.A., 1991. *Elements of Information Theory*, 2nd ed, John Wiley & Sons.
- Fahrmeir, L., Tutz, G., 2001. *Multivariate Statistical Modelling Based on Generalized Linear Models*, Springer Series in Statistics. Springer New York, New York, NY.  
<https://doi.org/10.1007/978-1-4757-3454-6>
- Fernandez, B., Salas, J.D., 1990. Gamma-Autoregressive Models for Stream-Flow Simulation. *J. Hydraul. Eng.* 116, 1403–1414. [https://doi.org/10.1061/\(asce\)0733-9429\(1990\)116:11\(1403\)](https://doi.org/10.1061/(asce)0733-9429(1990)116:11(1403))
- Frischkorn, H., Araújo, J.C., Santiago, M.M.F., 2003. Water Resources of Ceará and Piauí, in: *Global Change and Regional Impacts*. Springer Berlin Heidelberg, pp. 87–94.  
[https://doi.org/10.1007/978-3-642-55659-3\\_6](https://doi.org/10.1007/978-3-642-55659-3_6)
- Furrer, E., Katz, R., 2007. Generalized linear modeling approach to stochastic weather generators. *Clim. Res.* 34, 129–144. <https://doi.org/10.3354/cr034129>
- Hao, Z., Singh, V.P., 2011. Single-site monthly streamflow simulation using entropy theory. *Water Resour. Res.* 47. <https://doi.org/10.1029/2010WR010208>
- Hao, Z., Singh, V.P., 2013. Modeling multisite streamflow dependence with maximum entropy copula. *Water Resour. Res.* 49, 7139–7143. <https://doi.org/10.1002/wrcr.20523>
- Hao, Z., Singh, V.P., 2015. Integrating entropy and copula theories for hydrologic modeling and analysis. *Entropy* 17, 2253–2280. <https://doi.org/10.3390/e17042253>
- Hao, Z., Singh, V.P., 2016. Review of dependence modeling in hydrology and water resources. *Prog. Phys. Geogr. Earth Environ.* 40, 549–578.  
<https://doi.org/10.1177/0309133316632460>
- Huang, C.Y., Zhang, Y.P., 2019. Prediction based on copula entropy and general regression neural network. *Appl. Ecol. Environ. Res.* 17, 14415–14424.  
[https://doi.org/10.15666/aeer/1706\\_1441514424](https://doi.org/10.15666/aeer/1706_1441514424)
- Joe, H., 1997. *Multivariate Models and Multivariate Dependence Concepts*, Multivariate Models and Multivariate Dependence Concepts. Chapman and Hall/CRC.  
<https://doi.org/10.1201/9780367803896>
- Joe, H., 2014. *Dependence modeling with copulas*, Dependence Modeling with Copulas. CRC Press. <https://doi.org/10.1201/b17116>
- Kao, S.C., Govindaraju, R.S., 2008. Trivariate statistical analysis of extreme rainfall events via the Plackett family of copulas. *Water Resour. Res.* 44.  
<https://doi.org/10.1029/2007WR006261>

- Kleiber, W., Katz, R.W., Rajagopalan, B., 2012. Daily spatiotemporal precipitation simulation using latent and transformed Gaussian processes. *Water Resour. Res.* 48. <https://doi.org/10.1029/2011WR011105>
- Krupskii, P., Joe, H., 2015. Tail-weighted measures of dependence. *J. Appl. Stat.* 42, 614–629. <https://doi.org/10.1080/02664763.2014.980787>
- Lall, U., Sharma, A., 1996. A nearest neighbor bootstrap for resampling hydrologic time series. *Water Resour. Res.* 32, 679–693. <https://doi.org/10.1029/95WR02966>
- Lee, T., Salas, J.D., 2008. Using Copulas for Stochastic Streamflow Generation, in: *World Environmental and Water Resources Congress 2008*. American Society of Civil Engineers, Reston, VA, pp. 1–10. [https://doi.org/10.1061/40976\(316\)572](https://doi.org/10.1061/40976(316)572)
- Lee, T., Salas, J.D., 2011. Copula-based stochastic simulation of hydrological data applied to Nile River flows. *Hydrol. Res.* 42, 318–330. <https://doi.org/10.2166/nh.2011.085>
- Ma, J., 2020. copent: Estimating Copula Entropy in R. R package version 0.1. <https://CRAN.R-project.org/package=copent>
- Ma, J., Sun, Z., 2011. Mutual Information Is Copula Entropy. *TSINGHUA Sci. Technol.* 16, 51–54. [https://doi.org/10.1016/S1007-0214\(11\)70008-6](https://doi.org/10.1016/S1007-0214(11)70008-6)
- McCullagh, P., Nelder, J.A., 1989. *Generalized Linear Models*, 2nd ed. Chapman and Hall/CRC. <https://doi.org/10.1201/9780203753736>
- McMahon, T.A., Adedoye, A.J., Zhou, S.L., 2006. Understanding performance measures of reservoirs. *J. Hydrol.* 324, 359–382. <https://doi.org/10.1016/j.jhydrol.2005.09.030>
- Moura, A.D., Shukla, J., 1981. On the dynamics of droughts in northeast Brazil: observations, theory and numerical experiments with a general circulation model. *J. Atmos. Sci.* 38, 2653–2675. [https://doi.org/10.1175/1520-0469\(1981\)038<2653:OTDODI>2.0.CO;2](https://doi.org/10.1175/1520-0469(1981)038<2653:OTDODI>2.0.CO;2)
- Nelsen, R.B., 2006. *An Introduction to Copulas*, An Introduction to Copulas. Springer, New York. <https://doi.org/10.1007/0-387-28678-0>
- Ni, L., Wang, D., Wu, J., Wang, Y., Tao, Y., Zhang, J., Liu, J., Xie, F., 2020. Vine copula selection using mutual information for hydrological dependence modeling. *Environ. Res.* 186, 109604. <https://doi.org/10.1016/j.envres.2020.109604>
- Pereira, G.A.A., Veiga, Á., Erhardt, T., Czado, C., 2017. A periodic spatial vine copula model for multi-site streamflow simulation. *Electr. Power Syst. Res.* 152, 9–17. <https://doi.org/10.1016/j.epsr.2017.06.017>
- Prairie, J.R., Rajagopalan, B., Fulp, T.J., Zagana, E.A., 2006. Modified K-NN Model for Stochastic Streamflow Simulation. *J. Hydrol. Eng.* 11, 371–378.
- R Core Team, 2013. *R: A language and environment for statistical computing*. R Foundation for Statistical Computing, Vienna, Austria. ISBN 3-900051-07-0, URL <http://www.R-project.org/>

- Rajagopalan, B., Salas, J.D., Lall, U., 2010. Stochastic methods for modeling precipitation and streamflow, in: *Advances in Data-Based Approaches for Hydrologic Modeling and Forecasting*. World Scientific Publishing Co., pp. 17–52.  
[https://doi.org/10.1142/9789814307987\\_0002](https://doi.org/10.1142/9789814307987_0002)
- Robbins, N.B., 2004. *Creating More Effective Graphs*. John Wiley & Sons, Inc., Hoboken, NJ, USA. <https://doi.org/10.1002/9780471698180>
- Salas, J.D., 1993. Analysis and modeling of hydrologic time series. In: *Handbook of Hydrology* (D. R. Maidment ed.), McGraw-Hill, New York.
- Salas, J. D., Delleur, J. W., Yevjevich, V., and Lane, W. L., 1980. *Applied Modeling of Hydrologic Time Series*. Water Resources Publications, Littleton, Colorado.
- Salas, J.D., Lee, T., 2010. Nonparametric Simulation of Single-Site Seasonal Streamflows. *J. Hydrol. Eng.* 15, 284–296. [https://doi.org/10.1061/\(asce\)he.1943-5584.0000189](https://doi.org/10.1061/(asce)he.1943-5584.0000189)
- Schepsmeier, U., Stoeber, J., Brechmann, E. C., Graeler, B., Nagler, T., Erhardt, T., ... & Killiches, M., 2018. Package ‘VineCopula’. R package version, 2(5).
- Shannon, C.E., 1948. A Mathematical Theory of Communication. *Bell Syst. Tech. J.* 27, 623–656. <https://doi.org/10.1002/j.1538-7305.1948.tb00917.x>
- Sharma, A., O’Neill, R., 2002. A nonparametric approach for representing interannual dependence in monthly streamflow sequences. *Water Resour. Res.* 38, 5-1-5–10.  
<https://doi.org/10.1029/2001wr000953>
- Sharma, A., Tarboton, D.G., Lall, U., 1997. Streamflow simulation: A nonparametric approach. *Water Resour. Res.* 33, 291–308. <https://doi.org/10.1029/96WR02839>
- Silva, A.T., Portela, M.M., 2012. Disaggregation modelling of monthly streamflows using a new approach of the method of fragments. *Hydrol. Sci. J.* 57, 942–955.  
<https://doi.org/10.1080/02626667.2012.686695>
- Silva, S.M.O. da, Souza Filho, F. de A., Aquino, S.H.S., 2017. Avaliação do risco da alocação de água em período de escassez hídrica: o caso do Sistema Jaguaribe-Metropolitano. *Eng. Sanit. e Ambient.* 22, 749–760. <https://doi.org/10.1590/s1413-41522017161303>
- Singh, V.P., Zhang, L., 2018. Copula–entropy theory for multivariate stochastic modeling in water engineering. *Geosci. Lett.* 5. <https://doi.org/10.1186/s40562-018-0105-z>
- Sklar, M., 1959. Fonctions de repartition an dimensions et leurs marges. *Publ. inst. statist. univ. Paris*, 8, 229-231.
- Spliid, H., 2017. marima: Multivariate ARIMA and ARIMA-X Analysis. R package version 2.2. <https://CRAN.R-project.org/package=marima>
- Souza Filho, F.A., Lall, U., 2003. Seasonal to interannual ensemble streamflow forecasts for Ceara, Brazil: Applications of a multivariate, semiparametric algorithm. *Water Resour. Res.* 39. <https://doi.org/10.1029/2002WR001373>

- Srinivas, V. V., Srinivasan, K., 2005. Hybrid moving block bootstrap for stochastic simulation of multi-site multi-season streamflows. *J. Hydrol.* 302, 307–330. <https://doi.org/10.1016/j.jhydrol.2004.07.011>
- Srivastav, R.K., Simonovic, S.P., 2014. An analytical procedure for multi-site, multi-season streamflow generation using maximum entropy bootstrapping. *Environ. Model. Softw.* 59, 59–75. <https://doi.org/10.1016/j.envsoft.2014.05.005>
- Sun, F., Zhang, Wendi, Wang, N., Zhang, Wei, 2019. A copula entropy approach to dependence measurement for multiple degradation processes. *Entropy* 21. <https://doi.org/10.3390/e21080724>
- Verdin, A., Rajagopalan, B., Kleiber, W., Katz, R.W., 2014. Coupled stochastic weather generation using spatial and generalized linear models. *Stoch. Environ. Res. Risk Assess.* 29, 347–356. <https://doi.org/10.1007/s00477-014-0911-6>
- Wang, W., Dong, Z., Lall, U., Dong, N., Yang, M., 2019. Monthly Streamflow Simulation for the Headwater Catchment of the Yellow River Basin With a Hybrid Statistical-Dynamical Model. *Water Resour. Res.* 55, 7606–7621. <https://doi.org/10.1029/2019WR025103>
- Wang, X., Auler, A.S., Edwards, R.L., Cheng, H., Cristalli, P.S., Smart, P.L., Richards, D.A., Shen, C.-C., 2004. Wet periods in northeastern Brazil over the past 210 kyr linked to distant climate anomalies. *Nature* 432, 740–743. <https://doi.org/10.1038/nature03067>
- Wheater, H.S., Chandler, R.E., Onof, C.J., Isham, V.S., Bellone, E., Yang, C., Lekkas, D., Lourmas, G., Segond, M.L., 2005. Spatial-temporal rainfall modelling for flood risk estimation. *Stoch. Environ. Res. Risk Assess.* 19, 403–416. <https://doi.org/10.1007/s00477-005-0011-8>
- Yang, C., Chandler, R.E., Isham, V.S., Wheeler, H.S., 2005. Spatial-temporal rainfall simulation using generalized linear models. *Water Resour. Res.* 41, 1–13. <https://doi.org/10.1029/2004WR003739>
- Zachariah, M., Reddy, M.J., 2013. Development of an entropy-copula-based stochastic simulation model for generation of monthly inflows into the Hirakud Dam. *ISH J. Hydraul. Eng.* 19, 267–275. <https://doi.org/10.1080/09715010.2013.804697>
- Zhao, N., Lin, W.T., 2011. A copula entropy approach to correlation measurement at the country level. *Appl. Math. Comput.* 218, 628–642.
- Ávila, L., Silveira, R., Campos, A., Rogiski, N., Freitas, C., Aver, C., & Fan, F. (2023). Seasonal Streamflow Forecast in the Tocantins River Basin, Brazil: An Evaluation of ECMWF-SEAS5 with Multiple Conceptual Hydrological Models. *Water*, 15(9), 1695.
- Becker, E., Kirtman, B. P., & Pegion, K. (2020). Evolution of the North American multi-model ensemble. *Geophysical Research Letters*, 47, e2020GL087408. <https://doi.org/10.1029/2020GL087408>
- Becker, E. J., Kirtman, B. P., L'Heureux, M., Muñoz, Á. G., & Pegion, K. (2022). A decade of

the North American Multimodel Ensemble (NMME): Research, application, and future directions. *Bulletin of the American Meteorological Society*, 103(3), E973-E995.

Block, P. J., Souza Filho, F. A., Sun, L., & Kwon, H. H. (2009). A streamflow forecasting framework using multiple climate and hydrological models 1. *JAWRA Journal of the American Water Resources Association*, 45(4), 828-843.

Boucher, M. A., Tremblay, D., Delorme, L., Perreault, L., & Anctil, F. (2012). Hydro-economic assessment of hydrological forecasting systems. *Journal of Hydrology*, 416, 133-144.

Cao, Q., Shukla, S., DeFlorio, M. J., Ralph, F. M., & Lettenmaier, D. P. (2021). Evaluation of the subseasonal forecast skill of floods associated with atmospheric rivers in coastal Western US watersheds. *Journal of Hydrometeorology*, 22(6), 1535-1552.

Cassagnole, M., Ramos, M. H., Zalachori, I., Thirel, G., Garçon, R., Gailhard, J., & Ouillon, T. (2021). Impact of the quality of hydrological forecasts on the management and revenue of hydroelectric reservoirs—a conceptual approach. *Hydrology and Earth System Sciences*, 25(2), 1033-1052.

Cavalcante, M. R. G., da Cunha Luz Barcellos, P., & Cataldi, M. (2020). Flash flood in the mountainous region of Rio de Janeiro state (Brazil) in 2011: part I—calibration watershed through hydrological SMAP model. *Natural Hazards*, 102, 1117-1134.

Fan, F. M., Schwanenberg, D., Alvarado, R., Assis dos Reis, A., Collischonn, W., & Nauman, S. (2016). Performance of deterministic and probabilistic hydrological forecasts for the short-term optimization of a tropical hydropower reservoir. *Water Resources Management*, 30, 3609-3625.

Fan, F. M., Schwanenberg, D., Collischonn, W., & Weerts, A. (2015). Verification of inflow into hydropower reservoirs using ensemble forecasts of the TIGGE database for large scale basins in Brazil. *Journal of Hydrology: Regional Studies*, 4, 196-227.

Feng, P. N., Lin, H., Derome, J., & Merlis, T. M. (2021). Forecast skill of the NAO in the subseasonal-to-seasonal prediction models. *Journal of Climate*, 34(12), 4757-4769.

Greuell, W., & Hutjes, R. W. (2023). Skill and sources of skill in seasonal streamflow hindcasts for South America made with ECMWF's SEAS5 and VIC. *Journal of Hydrology*, 617, 128806.

IRI, International Research Institute. "Descriptions of the IRI Climate Forecast Verification Scores.", 2013.

Jiang, X., Adames, Á. F., Kim, D., Maloney, E. D., Lin, H., Kim, H., ... & Klingaman, N. P. (2020). Fifty years of research on the Madden-Julian Oscillation: Recent progress, challenges, and perspectives. *Journal of Geophysical Research: Atmospheres*, 125(17), e2019JD030911.

Kwon, H. H., de Assis de Souza Filho, F., Block, P., Sun, L., Lall, U., & Reis Jr, D. S. (2012). Uncertainty assessment of hydrologic and climate forecast models in Northeastern Brazil.



*Hydrological Processes*, 26(25), 3875-3885.

Lopes, J.E.G.; Braga, B., Jr.; Conejo, J. SMAP—A simplified hydrologic model. In *Applied Modeling in Catchment Hydrology*; Singh, V.P., Ed.; Water Resources Publications: Littleton, CO, USA, 1982.

Matte, S., Boucher, M. A., Boucher, V., & Fortier Fillion, T. C. (2017). Moving beyond the cost–loss ratio: economic assessment of streamflow forecasts for a risk-averse decision maker. *Hydrology and Earth System Sciences*, 21(6), 2967-2986.

McInerney, D., Thyer, M., Kavetski, D., Laugesen, R., Woldemeskel, F., Tuteja, N., and Kuczera, G.: Seamless streamflow forecasting at daily to monthly scales: MuTHRE lets you have your cake and eat it too, *Hydrol. Earth Syst. Sci.*, 26, 5669–5683, <https://doi.org/10.5194/hess-26-5669-2022>, 2022.

McInerney, D., Thyer, M., Kavetski, D., Laugesen, R., Tuteja, N., & Kuczera, G. (2020). Multi-temporal hydrological residual error modeling for seamless subseasonal streamflow forecasting. *Water Resources Research*, 56, e2019WR026979. <https://doi.org/10.1029/2019WR026979>

MORIASI, D. N.; ARNOLD, J. G.; LIEW, M. W. Van; BINGNER, R. L.; HARMEL, R. D.; VEITH, T. L. Model evaluation guidelines for systematic quantification of accuracy in watershed simulations. *Transactions of the ASABE*, [S. l.], v. 50, n. 3, p. 885–900, 2007.

Najafi, Mohammad Reza, and Hamid Moradkhani. "Ensemble combination of seasonal streamflow forecasts." *Journal of Hydrologic Engineering* 21.1 (2016): 04015043.

ONS, Operador Nacional do Sistema Elétrico, 2012. Available in [www.ons.org.br](http://www.ons.org.br).

Panahi, F., Ehteram, M., Ahmed, A. N., Huang, Y. F., Mosavi, A., & El-Shafie, A. (2021). Streamflow prediction with large climate indices using several hybrid multilayer perceptrons and copula Bayesian model averaging. *Ecological Indicators*, 133, 108285.

Pegion, K., Kirtman, B. P., Becker, E., Collins, D. C., LaJoie, E., Burgman, R., ... & Kim, H. (2019). The Subseasonal Experiment (SubX): A multimodel subseasonal prediction experiment. *Bulletin of the American Meteorological Society*, 100(10), 2043-2060.

Prado Jr, F. A., Athayde, S., Mossa, J., Bohlman, S., Leite, F., & Oliver-Smith, A. (2016). How much is enough? An integrated examination of energy security, economic growth and climate change related to hydropower expansion in Brazil. *Renewable and Sustainable Energy Reviews*, 53, 1132-1136.

Porto, V. C., de Souza Filho, F. D. A., Carvalho, T. M. N., de Carvalho Studart, T. M., & Portela, M. M. (2021). A GLM copula approach for multisite annual streamflow generation. *Journal of Hydrology*, 598, 126226.

Quedi, E. S., & Fan, F. M. (2020). Sub seasonal streamflow forecast assessment at large-scale



basins. *Journal of Hydrology*, 584, 124635.

Robertson, Andrew W., et al. "Improved combination of multiple atmospheric GCM ensembles for seasonal prediction." *Monthly Weather Review* 132.12 (2004): 2732-2744.

Sankarasubramanian, A., Lall, U., Souza Filho, F. A., & Sharma, A. (2009). Improved water allocation utilizing probabilistic climate forecasts: Short-term water contracts in a risk management framework. *Water Resources Research*, 45(11)

Souza Filho, Francisco Assis, and Upmanu Lall. "Seasonal to interannual ensemble streamflow forecasts for Ceara, Brazil: Applications of a multivariate, semiparametric algorithm." *Water Resources Research* 39.11 (2003).

SOUZA FILHO, Francisco de Assis de; LALL, Upmanu. Modelo de previsão de vazões sazonais e interanuais. RBRH - Revista Brasileira de Recursos Hídricos, [S. l.], v. 9, n. 2, p. 61-74, 2004.

Tebaldi, Claudia, and Reto Knutti. "The use of the multi-model ensemble in probabilistic climate projections." *Philosophical transactions of the royal society A: mathematical, physical and engineering sciences* 365.1857 (2007): 2053-2075.

Tiwari, A. D., & Mishra, V. (2022). Sub-seasonal prediction of drought and streamflow anomalies for water management in India. *Journal of Geophysical Research: Atmospheres*, 127, e2021JD035737. <https://doi.org/10.1029/2021JD035737>

Weigel, Andreas P., M. A. Liniger, and C. Appenzeller. "Can multi-model combination really enhance the prediction skill of probabilistic ensemble forecasts?." *Quarterly Journal of the Royal Meteorological Society: A journal of the atmospheric sciences, applied meteorology and physical oceanography* 134.630 (2008): 241-260.

Zhou, Y., Zaitchik, B. F., Kumar, S. V., Arsenault, K. R., Matin, M. A., Qamer, F. M., ... & Shakya, K. (2021). Developing a hydrological monitoring and sub-seasonal to seasonal forecasting system for South and Southeast Asian river basins. *Hydrology and Earth System Sciences*, 25(1), 41-61.

